Chapter 13

Solution of the One Dimensional Euler Equations

13.1 Introduction

The one dimensional shock tube problem has been used frequently in Chapters 9 and 10 to illustrate algorithms for solving the Euler equations. Here we will solve both the unsteady Quasi 1-D Euler equations described in Section 7.5.1 and the steady Euler equations described in Section 2.7.2. Five initial value problems will be solved , (1) flow within a supersonic inlet, (2) flow within a converging- diverging nozzle, (3) flow within a piston cylinder, (4) flow over an expansion surface and (5) flow past a compression surface.. These problems were chosen to illustrate the application of algorithms and boundary condition procedures discussed in the preceding chapters.

We begin with the Quasi 1-D Euler equations given below.

$$\frac{\partial U}{\partial t}+\frac{1}{S}\frac{\partial FS}{\partial x}=Q$$

where

$$U=\begin{bmatrix}\rho\\ \rho u\\ e\end{bmatrix},\quad F=\begin{bmatrix}\rho u\\ \rho u^2+p\\ (e+p)u\end{bmatrix},\quad and\quad Q=\begin{bmatrix}0\\ \dfrac{p}{S}\dfrac{\partial S}{\partial x}\\ 0\end{bmatrix}$$

$$p=(\gamma-1)\rho\varepsilon,\quad \varepsilon=\frac{e}{\rho}-\frac{1}{2}u^2\quad and\quad S=S(x)$$

For purely one dimensional flow $S(x)\equiv 1$ and $Q=\left[0,0,0\right]^T$

13.2The Supersonic Inlet Problem

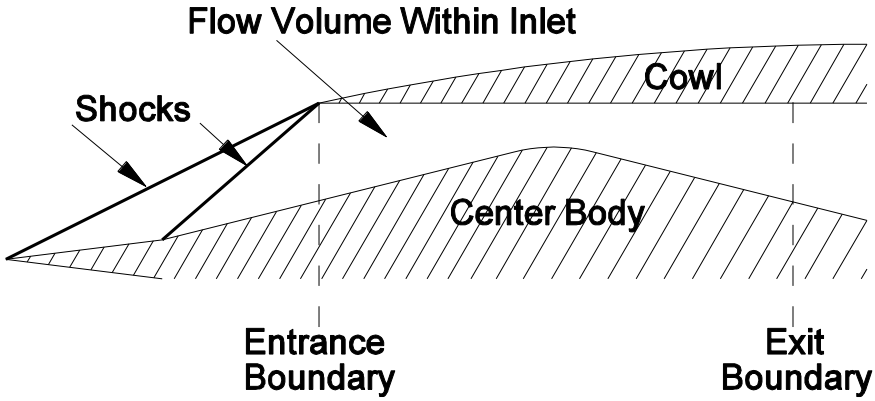

Figure 13.1 Flow within a supersonic inlet

Exercise (1): Calculate the flow within the supersonic inlet shown above. Solve the Quasi 1-D Euler equations with an implicit method. Choose either the Modified Steger-Warming or Roe methods.

Inlet Geometry

At the entrance and exit S equals $0.2m$. The lower surface of the channel is formed by two straight lines inclined at angle θ, given by $\tan\theta = 0.25$, with their intersection at the channel midpoint rounded out with a radius equal to $0.5m$.

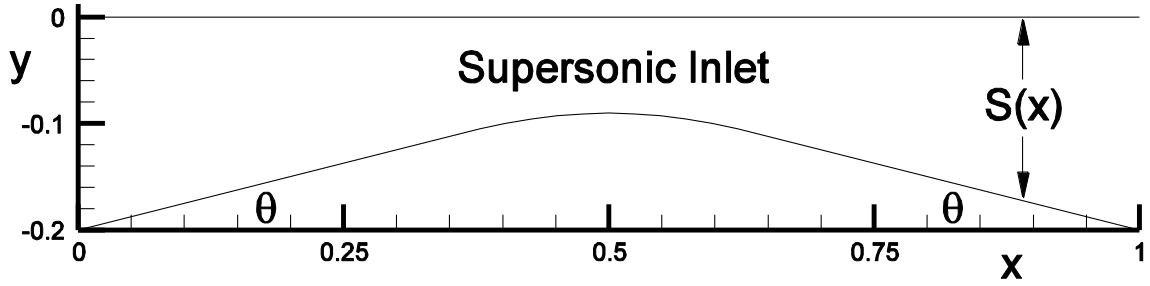

Figure 13.2 Inlet geometry

Computational Mesh

Use 41 equally spaced mesh points located along the line $y = 0$ or 40 equally spaced volumes, as shown below, to span the flow volume.

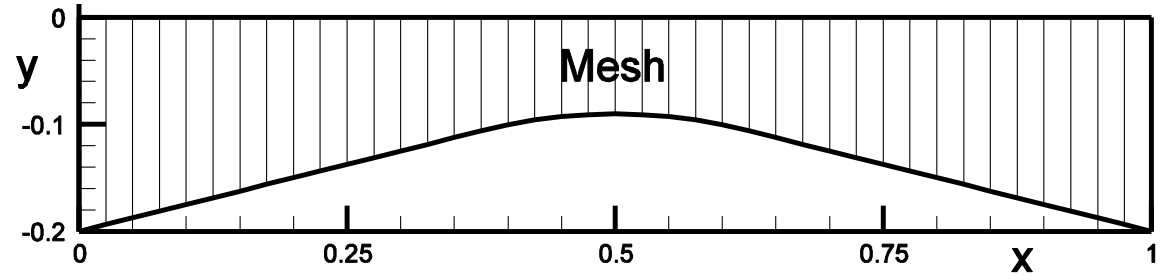

Figure 13.3 Computational mesh

Cases

Run each case below for 200 time steps. Show flow field results for surface pressure vs. x initially and for every 40 time steps.

1) No Flow Case - $M_0 = 0$, $p_0 = 1\times10^6\ N/m^2$ and $T_0 = 300^o K$ everywhere. Use $\Delta t = \left.\dfrac{\Delta x}{u+c}\right|_1$

2) No Shock Wave Case - $M_0 = 2.5$, $p_0 = 1\times10^6\ N/m^2$ and $T_0 = 300^o K$ at the entrance. Use isentropic relations to initialize the flow downstream of the entrance to the exit. Use $\Delta t = 2\left.\dfrac{\Delta x}{u+c}\right|_1$.

3) Stationary Shock Wave Case, - Use the same initial conditions as in Case (2), but place a shock wave at $x = 0.85m$. Use $\Delta t = 2\dfrac{\Delta x}{u+c}\bigg|_1$.

4) Moving Shock Case – Start with the solution from Case (3) and then increase the exit pressure by 67% ($p_{exit} \leftarrow 1.67 \times p_{exit}$) initially and thereafter hold it fixed. Use $\Delta t = \dfrac{\Delta x}{u+c}\bigg|_1$

13.2.1 Solution Approach

Initial Conditions

The purpose of Case (1) is to check, during the early development of the computer program, that no acceleration is produced within a zero pressure gradient flow field. This is a preliminary check on the flux balance for pressure about each flow volume. Isentropic relations can be used to create the initial flow field for Case (2). First, (see Anderson - *Fundamentals of Aerodynamics*) the following relationship between channel area and Mach number can be solved for M, using Newton's method for any $A = S(x)$, with A_0 and M_0 taken at the entrance at $x = 0$.

$$\left(\frac{A}{A_0}\right)^2 = \left(\frac{M_0}{M}\right)^2 \left(\frac{1+\dfrac{\gamma-1}{2}M^2}{1+\dfrac{\gamma-1}{2}M_0^2}\right)^{\frac{\gamma+1}{\gamma-1}}$$

Newton's method was used in Section 5.3.1. In the present application we need to define the function for which we want M to satisfy such that $f(M) = 0$ at each x location.

$$f(M) = \left(\frac{A}{A_0}\right)^2 - \left(\frac{M_0}{M}\right)^2 \left(\frac{1+\dfrac{\gamma-1}{2}M^2}{1+\dfrac{\gamma-1}{2}M_0^2}\right)^{\frac{\gamma+1}{\gamma-1}}$$

We can then obtain density, pressure and velocity at each x location, after M is found, using

$$\frac{\rho}{\rho_0} = \left(\frac{1+\dfrac{\gamma-1}{2}M_0^2}{1+\dfrac{\gamma-1}{2}M^2}\right)^{\frac{1}{\gamma-1}}, \quad \frac{p}{p_0} = \left(\frac{1+\dfrac{\gamma-1}{2}M_0^2}{1+\dfrac{\gamma-1}{2}M^2}\right)^{\frac{\gamma}{\gamma-1}} \quad \text{and} \quad u = \frac{\rho_0 A_0}{\rho A}u_0$$

The Case (2) initial conditions for density, velocity and pressure are shown in the figure below.

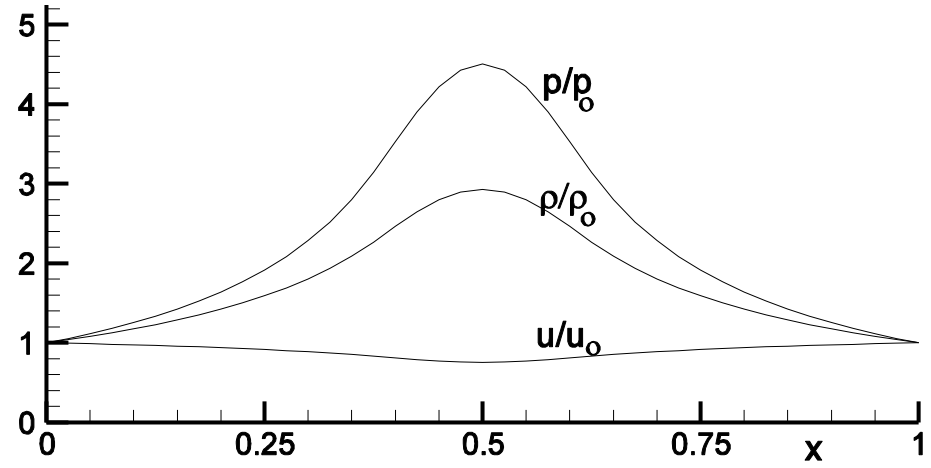

Figure 13.4 Initial condition for Case (2)

We need to place a shock wave at $x = 0.85m$ for Case (3). First, the isentropic relations are solved for $x \le 0.85m$, as given above. At $x = 0.85m$ the jump relations for a stationary shock wave in one dimension given Section 2.4.3.7 are solved, using the known values for density ρ_1, velocity u_1, pressure p_1 and total energy e_1, for the values ρ_2, u_2, p_2 and e_2 behind the shock wave, also at $x = 0.85m$. The isentropic relations can then be used again to determine the solution downstream of the shock, but first they must be reinitialized by the flow values just downstream of the shock wave. That is, downstream of the shock the following replacements are used.

$$A_0 \leftarrow S|_{x=0.85m},\ M_0 \leftarrow M_2 = u_2 / \sqrt{\frac{\gamma p_2}{\rho_2}},\ u_0 \leftarrow u_2,\ \rho_0 \leftarrow \rho_2 \text{ and } p_0 \leftarrow p_2 .$$

The initial condition for Case (3) is shown below

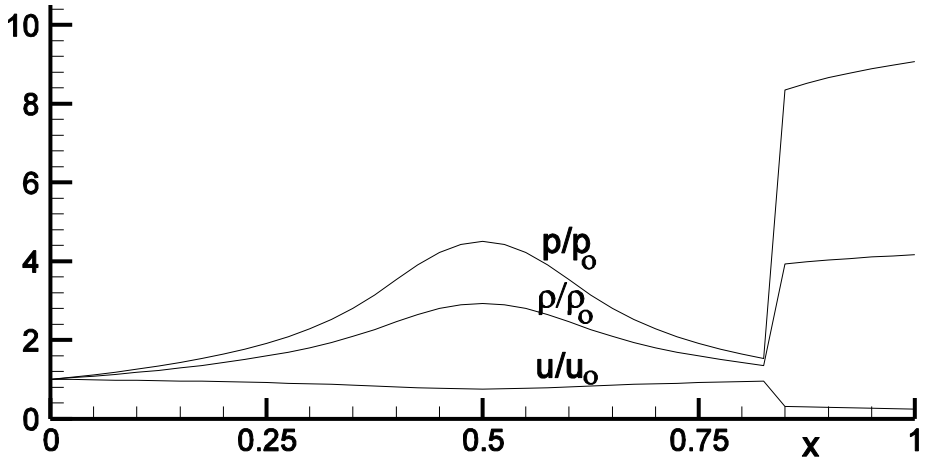

Figure 13.5 Initial condition for Case (3)

The initial condition for Case (4) modifies the initial condition used for Case (3) at the exit by increasing the pressure by 67%, $\delta p = 0.67\, p_{exit}$. This is sufficient to cause the shock wave to move forward past the channel throat. Related isentropic changes to density and velocity should also be made at the exit as follows. The exit conditions are then held fixed during the calculation.

$$p_{exit} \leftarrow p_{exit} + \delta p\,, \quad \rho_{exit} \leftarrow \rho_{exit} + \frac{\delta p}{c^2} \quad \text{and} \quad u_{exit} = \frac{\rho_0 A_0}{\rho_{exit} A_{exit}} u_0$$

13.2.2 Boundary Conditions

See Section 12.3-5 for a discussion on entrance and exit boundary conditions. For the present flow problem of the supersonic inlet, the entrance boundary is located within a region of supersonic flow. Therefore, the conditions at the entrance are held fixed in time at their initial values.

$$U_1^n = U\big|_{x=0}^{t=0} \quad \text{and} \quad \delta U_1^{n+1} = 0$$

The flow at the exit boundary can be either subsonic or supersonic. Boundary conditions for this type are discussed in Section 12.5. The conditions presented there can be modified for the Quasi 1-D Euler equations. The characteristic equations become

$$1)\ \frac{\partial \rho}{\partial t} - \frac{1}{c^2}\frac{\partial p}{\partial t} = -u\left(\frac{\partial \rho}{\partial x} - \frac{1}{c^2}\frac{\partial p}{\partial x}\right) \qquad .$$

$$2)\ \frac{\partial p}{\partial t} + \rho c \frac{\partial u}{\partial t} = -(u+c)\left(\frac{\partial p}{\partial x} + \rho c \frac{\partial u}{\partial x}\right) - \gamma p \frac{u}{S}\frac{\partial S}{\partial x}$$

$$3)\ \frac{\partial p}{\partial t} - \rho c \frac{\partial u}{\partial t} = -(u-c)\left(\frac{\partial p}{\partial x} - \rho c \frac{\partial u}{\partial x}\right) - \gamma p \frac{u}{S}\frac{\partial S}{\partial x}$$

$$\text{or} \quad \frac{\partial p}{\partial t} \ \text{ given at exit if } \ M_{exit} < 1$$

These characteristic equations can be approximated by either semi-implicit or fully implicit difference equations, discussed earlier in Section 12.5. We first apply the simpler semi-implicit approximation. Fully implicit boundary conditions for the Quasi 1-D Euler equations are discussed later in Section 13.2.5.

13.2.2.1 Semi-Implicit Boundary Condition at the Exit

The semi-implicit boundary condition approximations, discussed in Section 12.5.1, can be applied to the quasi 1-D characteristic relations, as shown below.

$$\delta\rho - \frac{1}{c^2}\delta p = -\frac{\lambda_1}{1+\lambda_1}\left(\rho_I^n - \rho_{I-1}^n - \frac{1}{c^2}(p_I^n - p_{I-1}^n)\right) = R_1, \quad \lambda_1 = u\frac{\Delta t}{\Delta x}$$

$$\delta p + \rho c\, \delta u = -\frac{\lambda_2}{1+\lambda_2}\left(p_I^n - p_{I-1}^n + \rho c(u_I^n - u_{I-1}^n)\right) - \frac{\Delta t \gamma p u}{1+\lambda_2}\frac{S_I - S_{I-1}}{S_I \Delta x} = R_2, \quad \lambda_2 = (u+c)\frac{\Delta t}{\Delta x}$$

$$\delta p - \rho c\,\delta u = -\frac{\lambda_4}{1+\lambda_4}\left(p_I^n - p_{I-1}^n - \rho c(u_I^n - u_{I-1}^n)\right) - \frac{\Delta t \gamma p u}{1+\lambda_4}\frac{S_I - S_{I-1}}{S_I \Delta x} = R_4, \quad \lambda_4 = (u-c)\frac{\Delta t}{\Delta x}$$

Solving for δp

$$\delta p = \begin{cases} \dfrac{R_2 + R_4}{2}, & if \quad M = \dfrac{u_{I-1}}{c_{I-1}} > 1 \\ 0 \quad , & if \quad M < 1 \text{ (assuming } \dfrac{\partial \mathrm{p}_{\mathrm{exit}}}{\partial \mathrm{t}} = 0) \end{cases}$$

Then

$$\delta\rho = R_1 + \frac{\delta p}{c^2} \quad \text{and} \quad \delta u = \frac{R_2 - \delta p}{\rho c}$$

Therefore,

$$\rho_I^{n+1} = \rho_I^n + \delta\rho \qquad T_I^{n+1} = \frac{p_I^{n+1}}{(\gamma-1)c_v\rho_I^{n+1}} \quad \text{and}$$

$$u_I^{n+1} = u_I^n + \delta u$$

$$p_I^{n+1} = p_I^n + \delta p \qquad e_I^{n+1} = \rho_I^{n+1}\left(c_v T_I^{n+1} + \frac{1}{2}(u_I^{n+1})^2\right)$$

The conserved variable changes for density, momentum and energy at exit grid point I are

$$\delta U_I^{n+1} = \begin{bmatrix} \rho_I^{n+1} - \rho_I^n \\ \rho_I^{n+1}u_I^{n+1} - \rho_I^n u_I^n \\ e_I^{n+1} - e_I^n \end{bmatrix} = \bar{\mathrm{R}}_{\mathrm{I}}^{\mathrm{n+1}}$$

13.2.3 Solution Algorithm

The implicit solution algorithm for the Quasi 1-D Euler equations can be written as follows.

$$\left\{I + \frac{\Delta t}{S_i}\left(\frac{D_-\cdot}{\Delta x}S_{i+1/2}\bar{A}_{+i+1/2}^n + \frac{D_+\cdot}{\Delta x}S_{i-1/2}\bar{A}_{-i-1/2}^n\right) - \Delta t H_i^n\right\}\delta U_i^{n+1} = -\frac{\Delta t}{S_i}\left(\frac{S_{i+1/2}F_{i+1/2}^n - S_{i-1/2}F_{i-1/2}^n}{\Delta x}\right) + \Delta t Q_i^n$$

where $\quad S_i = \dfrac{S_{i+1/2} + S_{i-1/2}}{2}, \quad Q_i^n = \dfrac{1}{S_i}\dfrac{S_{i+1/2} - S_{i-1/2}}{\Delta x}\begin{bmatrix} 0 \\ p_i^n \\ 0 \end{bmatrix}$ and the Jacobian

$$H_i^n = \left.\frac{\partial Q}{\partial U}\right|_i^n = \frac{S_{i+1/2} - S_{i-1/2}}{S_i \Delta x}(\gamma - 1)\begin{bmatrix} 0 & 0 & 0 \\ \dfrac{u^2}{2} & -u & 1 \\ 0 & 0 & 0 \end{bmatrix}_i^n$$

The split Jacobians can be evaluated from those given in Section 9.6 by removing the third rows and columns from the matrices given there, because there is no y-momentum equation or variable v in the Quasi 1-D Euler equations. The data used to define their elements is determine by either an arithmetic average for the Modified-Steger-Warming method or a Roe average for the Roe method from mesh points located about each flux surface, $i+1/2$ or $i-1/2$, which is indicated by the "*bars*" on split the Jacobian matrices shown above. For the present equations

$$A = S^{-1} C_A^{-1} \begin{bmatrix} u & 0 & 0 \\ 0 & u+c & 0 \\ 0 & 0 & u-c \end{bmatrix} C_A S \quad \text{where}$$

$$S = \begin{bmatrix} 1 & 0 & 0 \\ -u/\rho & 1/\rho & 0 \\ \alpha\beta & -u\beta & \beta \end{bmatrix}, \quad S^{-1} = \begin{bmatrix} 1 & 0 & 0 \\ u & \rho & 0 \\ \alpha & \rho u & 1/\beta \end{bmatrix},$$

$$C_A = \begin{bmatrix} 1 & 0 & -1/c^2 \\ 0 & \rho c & 1 \\ 0 & -\rho c & 1 \end{bmatrix}, \quad C_A^{-1} = \begin{bmatrix} 1 & \dfrac{1}{2c^2} & \dfrac{1}{2c^2} \\ 0 & \dfrac{1}{2\rho c} & \dfrac{-1}{2\rho c} \\ 0 & 1/2 & 1/2 \end{bmatrix}, \text{ and with } \alpha = \frac{u^2}{2} \text{ and } \beta = \gamma - 1$$

13.2.3.1 Matrix Equation

The implicit equation above represents a block tridiagonal matrix equation, which is given below.

$$\overline{\mathrm{B}}_i \delta U_{i+1}^{n+1} + \overline{\mathrm{A}}_i \delta U_i^{n+1} + \overline{\mathrm{C}}_i \delta U_{i-1}^{n+1} = \Delta U_i^n = -\frac{\Delta t}{S_i}\left(\frac{S_{i+1/2} F_{i+1/2}^n - S_{i-1/2} F_{i-1/2}^n}{\Delta x} \right) + \Delta t Q_i^n$$

The 3x3 block element matrices $\overline{\mathrm{A}}_i$, $\overline{\mathrm{B}}_i$ and $\overline{\mathrm{C}}_i$ are

$$\overline{\mathrm{A}}_i = I + \frac{\Delta t}{S_i \Delta x}\left(S_{i+1/2} \overline{A}_{+_{i+1/2}}^n - S_{i-1/2} \overline{A}_{-_{i-1/2}}^n \right) - \Delta t H_i^n,$$

$$\overline{\mathrm{B}}_i = + \frac{\Delta t}{S_i \Delta x} S_{i+1/2} \overline{A}_{-_{i+1/2}}^n \quad \text{and} \quad \overline{\mathrm{C}}_i = - \frac{\Delta t}{S_i \Delta x} S_{i-1/2} \overline{A}_{+_{i-1/2}}^n$$

The matrix equation to be solved is

$$\begin{bmatrix} \bar{A}_I & \bar{C}_I & 0 & 0 & 0 & 0 & 0 \\ \bar{B}_{I-1} & \bar{A}_{I-1} & 0 & 0 & 0 & 0 & 0 \\ 0 & \ddots & \ddots & \ddots & 0 & 0 & 0 \\ 0 & 0 & \bar{B}_i & \bar{A}_i & \bar{C}_i & 0 & 0 \\ 0 & 0 & 0 & \ddots & \ddots & \ddots & 0 \\ 0 & 0 & 0 & 0 & \bar{B}_2 & \bar{A}_2 & \bar{C}_2 \\ 0 & 0 & 0 & 0 & 0 & \bar{B}_1 & \bar{A}_1 \end{bmatrix} \begin{bmatrix} \delta U_I^{n+1} \\ \vdots \\ \delta U_{i+1}^{n+1} \\ \delta U_i^{n+1} \\ \delta U_{i-1}^{n+1} \\ \vdots \\ \delta U_1^{n+1} \end{bmatrix} = \begin{bmatrix} \Delta U_I^n \\ \vdots \\ \Delta U_{i+1}^n \\ \Delta U_i^n \\ \Delta U_{i-1}^n \\ \vdots \\ \Delta U_1^n \end{bmatrix}.$$

where the entrance boundary condition given earlier requires $\bar{A}_1 = I$, $\bar{B}_1 = 0$ and $\Delta U_1^n = 0$ and the exit boundary condition requires $\bar{A}_I = I$, $\bar{C}_I = 0$ and $\Delta U_I^n = \bar{R}_I^{n+1}$ (see the definition of $\bar{R}_I^{n+1}$ given earlier at the end of Section 13.2.2.1). The algorithm for solving this matrix equation is given in Section 11.3.

13.2.4 Solutions

Case (1) Solution

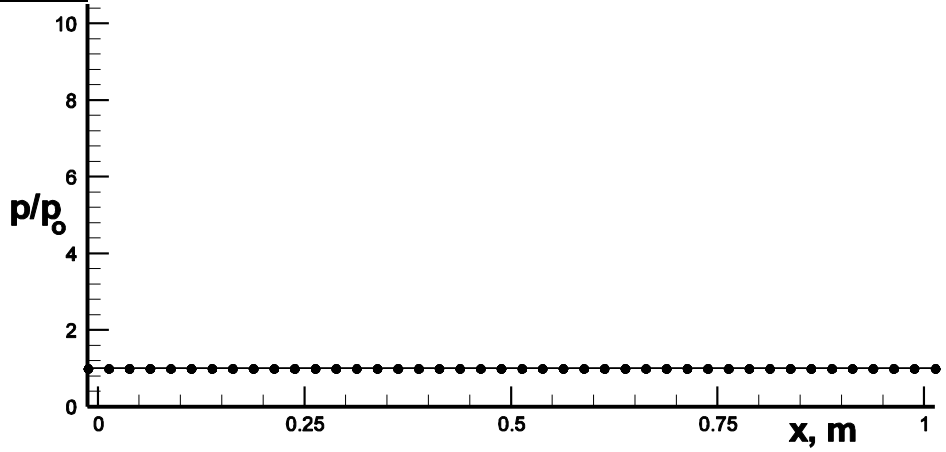

Figure 13.6 Case (1), no flow solution, 200 time steps

Case (2) Solution

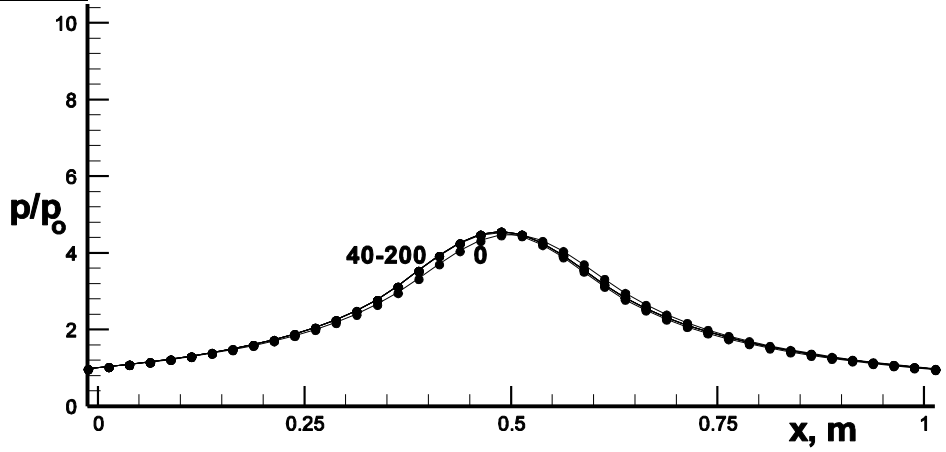

Figure 13.7 Case (2), no shock wave solution, 200 time steps

Case (3) Solution

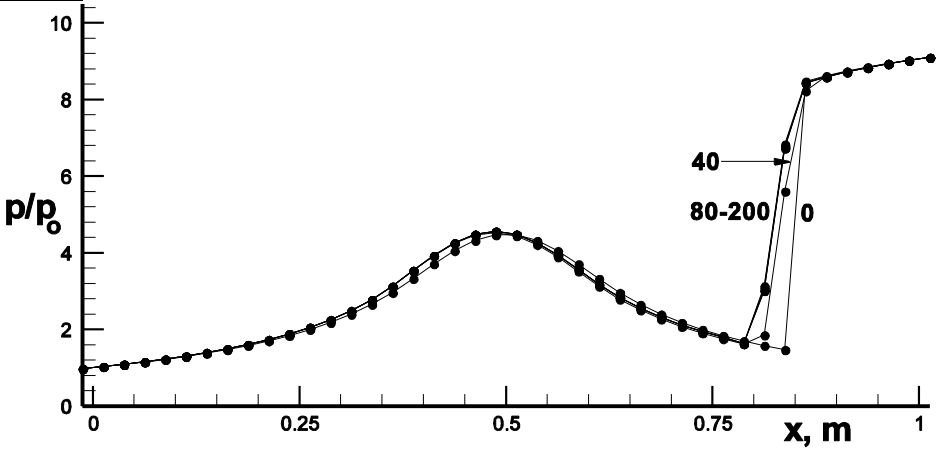

Figure 13.8 Case (3), stationary shock wave solution, 200 time steps

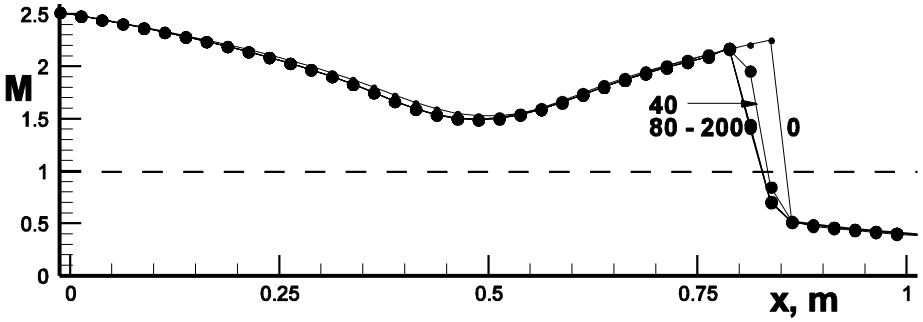

Figure 13.9 Case (3), stationary shock wave solution, Mach number vs. x

Case (4) Solution

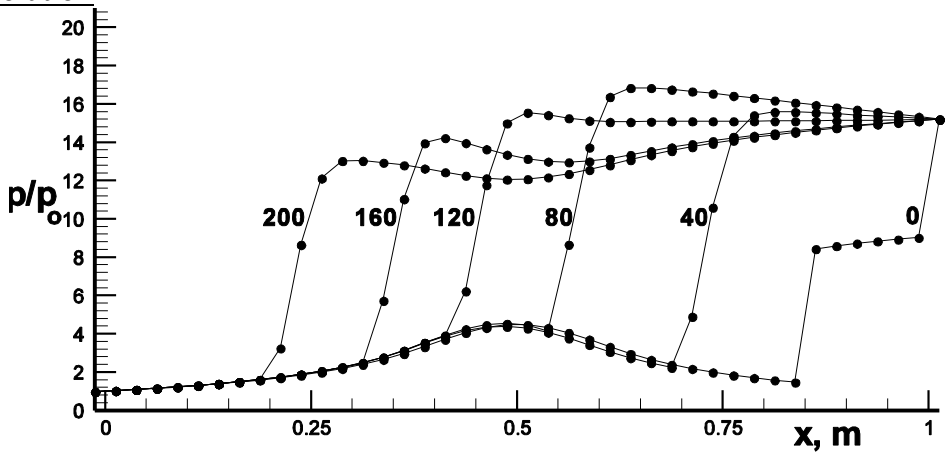

Figure 13.10 Case (4), moving shock wave solution, 200 time steps

Exercise (2): Repeat exercise (1), this time with fully implicit boundary conditions.

13.2.5 Fully Implicit Boundary Conditions

13.2.5.1 Exit Boundary Condition

Fully implicit boundary condition approximations, discussed in Section 12.5.2, can also be used for the quasi 1-D characteristic relations. The three characteristic equations given earlier can be written in matrix form as

$$C'\frac{\partial V}{\partial t} = -\Lambda C'\frac{\partial V}{\partial x} + Q', \quad \text{where} \quad C' = \begin{bmatrix} 1 & 0 & -1/c^2 \\ 0 & \rho c & 1 \\ 0 & -\rho c g & 1 \end{bmatrix},$$

$$\Lambda = \begin{bmatrix} u & 0 & 0 \\ 0 & u+c & 0 \\ 0 & 0 & (u-c)g \end{bmatrix},\ V = \begin{bmatrix} \rho \\ u \\ p \end{bmatrix},\ Q' = \begin{bmatrix} 0 \\ -\gamma p \dfrac{u}{S}\dfrac{\partial S}{\partial x} \\ -\gamma p \dfrac{u}{S}\dfrac{\partial S}{\partial x} g \end{bmatrix} \text{ and } g = \begin{cases} 1, \ if\ u \ge c \\ 0, \ if\ u < c \end{cases},$$

which assumes that the exit pressure is held fixed in time while the flow at the exit is subsonic. This equation can be approximated implicitly by

$$C'\frac{V_I^{n+1} - V_I^n}{\Delta t} = -\Lambda C'\frac{V_I^{n+1} - V_{I-1}^{n+1}}{\Delta x} + Q_I'^{n+1},$$

which in "delta " law form becomes

$$\left(C' + \frac{\Delta t}{\Delta x}\Lambda C' - \Delta t \left.\frac{\partial Q'}{\partial V}\right|_I^n \right)\delta V_I^{n+1} - \frac{\Delta t}{\Delta x}\Lambda C'\delta V_{I-1}^{n+1} = -\Delta t \Lambda C'\frac{V_I^n - V_{I-1}^n}{\Delta x} + \Delta t Q_I'^n$$

Using the matrix S given earlier to transform from δV to δU, we obtain

$$\left(C' + \frac{\Delta t}{\Delta x}\Lambda C' - \Delta t \left.\frac{\partial Q'}{\partial V}\right|_I^n \right) S\delta U_I^{n+1} - \frac{\Delta t}{\Delta x}\Lambda C' S\delta U_{I-1}^{n+1} = -\Delta t \Lambda C'\frac{V_I^n - V_{I-1}^n}{\Delta x} + \Delta t Q_I'^n$$

Therefore, we can now redefine the top row matrix equation elements, given in Section 13.2.3.1, for the fully implicit boundary condition as

$$\bar{\mathrm{A}}_I = \left(C' + \frac{\Delta t}{\Delta x}\Lambda C' - \Delta t \left.\frac{\partial Q'}{\partial V}\right|_I^n \right) S, \quad \bar{\mathrm{C}}_I = -\frac{\Delta t}{\Delta x}\Lambda C' S \quad \text{and} \quad \Delta U_I^n = -\Delta t \Lambda C'\frac{V_I^n - V_{I-1}^n}{\Delta x} + \Delta t Q_I'^n$$

13.2.5.2 Subsonic Entrance Boundary Conditions

There are two frequently used boundary condition types at subsonic entrances, (1) total pressure and temperature are specified and (2) total enthalpy and mass flow rate are specified. Any combination of two independent conditions will suffice, with the third piece of information required evaluated via a characteristic equation linking the boundary to the downstream flow.

Case (1) Total Pressure and Temperature Given at Entrance

If the flow at the entrance boundary is subsonic, $u_1 < c_1$, then from Section 12.4 two pieces of information concerning the flow would have to be prescribed from outside the flow and one characteristic equation would need to be solved. If the total pressure and temperature of the flow at the entrance were known, then the following equations would apply for quasi 1-D flow.

$$p = p_t\left[1-\frac{\gamma-1}{\gamma+1}\frac{u^2}{a_*^2}\right]^{\frac{\gamma}{\gamma-1}} = p(u)$$

$$T = T_t\left[1-\frac{\gamma-1}{\gamma+1}\frac{u^2}{a_*^2}\right] \quad = T(u)$$

$$\text{where} \quad a_*^2 = 2\gamma\frac{\gamma-1}{\gamma+1}c_v T_t\,.$$

$$\frac{\partial p}{\partial t}-\rho c\frac{\partial u}{\partial t} = -(u-c)\left(\frac{\partial p}{\partial x}-\rho c\frac{\partial u}{\partial x}\right)-\gamma p\frac{u}{S}\frac{\partial S}{\partial x}$$

From the first two equations above, we can obtain an equation for density as a function of u using the perfect gas equation of state.

$$\rho(u) = \frac{p(u)}{(\gamma-1)c_v T(u)}$$

We can differentiate this equation for $\rho(u)$ and the first equation for $p(u)$ with respect to u at $x_1 = 0$ to obtain the following two equations.

$$\delta\rho_1 = \left.\frac{\partial\rho}{\partial u}\right|_1 \delta u_1 \quad \text{and} \quad \delta p_1 = \left.\frac{\partial p}{\partial u}\right|_1 \delta u_1$$

The characteristic equation can be implicitly approximated as follows.

$$\frac{p_1^{n+1}-p_1^n}{\Delta t}-\rho c\,\frac{u_1^{n+1}-u_1^n}{\Delta t} = -(u-c)\left(\frac{p_2^{n+1}-p_1^{n+1}}{\Delta x}-\rho c\frac{u_2^{n+1}-u_1^{n+1}}{\Delta x}\right)-\gamma p_1^{n+1}u_1^{n+1}\frac{S_2-S_1}{S_1\Delta x}$$

This equation can be written in "delta" law form by expressing $p_i^{n+1} = p_i^n + \delta p_i$ and $u_i^{n+1} = u_i^n + \delta u_i$ and then retaining the lowest order terms.

$$\frac{\delta p_1}{\Delta t} - \rho c \frac{\delta u_1}{\Delta t} + (u-c)\left(\frac{\delta p_2 - \delta p_1}{\Delta x} - \rho c \frac{\delta u_2 - \delta u_1}{\Delta x} \right) + \gamma (u_1^n \delta p_1 + p_1^n \delta u_1) \frac{S_2 - S_1}{S_1 \Delta x} =$$

$$-(u-c)\left(\frac{p_2^n - p_1^n}{\Delta x} - \rho c \frac{u_2^n - u_1^n}{\Delta x} \right) - \gamma p_1^n u_1^n \frac{S_2 - S_1}{S_1 \Delta x} = R_3$$

Defining $\lambda_3 = (u-c)\dfrac{\Delta t}{\Delta x}$ and then combining the three equations for $\delta\rho$, δu and , δp we obtain the following matrix equation

$$\underbrace{\begin{bmatrix} 1 & -\left.\dfrac{\partial \rho}{\partial u}\right|_1 & 0 \\ 0 & -\left.\dfrac{\partial p}{\partial u}\right|_1 & 1 \\ 0 & -\rho c(1-\lambda_3) + \Delta t \gamma p_1^n \dfrac{S_2 - S_1}{S_1 \Delta x} & 1-\lambda_3 + \Delta t \gamma u_1^n \dfrac{S_2 - S_1}{S_1 \Delta x} \end{bmatrix}}_{A'} \delta V_1^{n+1} + \underbrace{\begin{bmatrix} 0 & 0 & 0 \\ 0 & 0 & 0 \\ 0 & -\rho c \lambda_3 & \lambda_3 \end{bmatrix}}_{B'} \delta V_2^{n+1} = \Delta t \underbrace{\begin{bmatrix} 0 \\ 0 \\ R_3 \end{bmatrix}}_{\bar{\mathrm{R}}}$$

Using the matrix S given earlier to transform from δV to δU, we obtain

$$A' S \delta U_1^{n+1} + B' S \delta U_2^{n+1} = \Delta t \bar{\mathrm{R}}$$

Therefore, if $u_1 < c_1$, we can now redefine the bottom row matrix equation elements given in Section 13.2.3.1 for the above fully implicit boundary condition by

$$\bar{\mathrm{A}}_1 = A'S, \quad \bar{\mathrm{B}}_1 = B'S \quad \text{and} \quad \Delta U_1^n = \Delta t \bar{\mathrm{R}}$$

<u>Case (2) Total Enthalpy and Mass flow Given at Entrance</u>

If total enthalpy, $h_t = (e+p)/\rho$, and mass flow rate, $m = \rho u$, are used to control the flow at the entrance, then we can replace the "delta" relations for total pressure and density used above as follows.

$$h_t = (e+p)/\rho = (\rho\varepsilon + \rho u^2/2 + p)/\rho,$$

where ε is the internal energy per unit mass and $\varepsilon = c_v T$. Using the perfect gas equation of state, $p = (\gamma - 1)\rho\varepsilon$, we obtain

$$h_t = \frac{\gamma}{\gamma-1}\frac{p}{\rho} + \frac{u^2}{2} \quad \text{and} \quad m = \rho u \qquad \text{The new "delta" relations are therefore}$$

$$\delta h_t = \frac{\gamma}{\gamma-1}\frac{\delta p}{\rho} - \frac{\gamma}{\gamma-1}\frac{p}{\rho^2}\delta\rho + u\delta u \quad \text{and} \quad \delta m = u\delta\rho + \rho\delta u$$

If total enthalpy and mass flow rate are fixed in time $\delta h_t = 0$ and $\delta m = 0$. The fully implicit boundary condition becomes

$$\underbrace{\begin{bmatrix} \rho & u & 0 \\ -\frac{\gamma}{\gamma-1}\frac{p}{\rho^2} & u & \frac{\gamma}{\gamma-1}\frac{1}{\rho} \\ 0 & -\rho c(1-\lambda_3)+\Delta t\gamma p_1^n \frac{S_2-S_1}{S_1\Delta x} & 1-\lambda_3+\Delta t\gamma u_1^n \frac{S_2-S_1}{S_1\Delta x} \end{bmatrix}}_{A'} \delta V_1^{n+1} + \underbrace{\begin{bmatrix} 0 & 0 & 0 \\ 0 & 0 & 0 \\ 0 & -\rho c\lambda_3 & \lambda_3 \end{bmatrix}}_{B'} \delta V_2^{n+1} = \Delta t \underbrace{\begin{bmatrix} \delta m \\ \delta h_t \\ R_3 \end{bmatrix}}_{\bar{\mathrm{R}}}$$

Again, if $u_1 < c_1$, we can redefine the bottom row matrix equation elements given in Section 13.2.3.1 for the above fully implicit boundary condition by

$$\bar{\mathrm{A}}_1 = A'S\,, \quad \bar{\mathrm{B}}_1 = B'S \quad \text{and} \quad \Delta U_1^n = \Delta t\bar{\mathrm{R}}$$

13.3 The Converging-Diverging Nozzle Problem

Exercise (3): Calculate the flow within a converging-diverging nozzle. Solve the Quasi 1-D Euler equations with an implicit method. Choose either the Modified Steger-Warming or Roe methods with Gauss-Seidel line relaxation.

Nozzle Geometry

The nozzle geometry is symmetric as shown in Figure 13.11. Therefore only the lower half of the flow within the nozzle needs to be calculated. The lower surface is formed by two straight lines joined smoothly together by an arc of a circle. The dimensions and angles are given below.

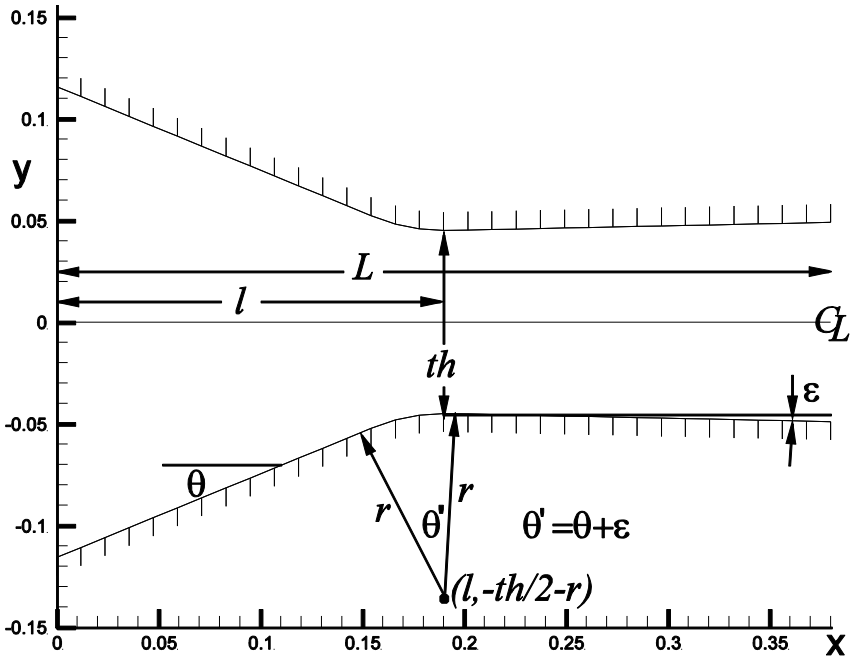

Figure 13.11 Converging-diverging nozzle geometry

$L = 0.38\,ft$, $l = 0.19\,ft$, $th = 0.09\,ft$, $r = 0.09\,ft$, $\theta = 22.33^o$ and $\varepsilon = 1.21^o$

Computational Mesh

Use 33 stretched mesh points spanning $0 \le x \le L$, or 34 finite volumes (with 2 boundary volumes), as shown below, to span the flow volume. Because of the flow symmetry only the volume below the center line need be calculated. The minimum Δx spacing is at the throat, where $\Delta x_{\min} = \dfrac{L}{2 \times 32}$.

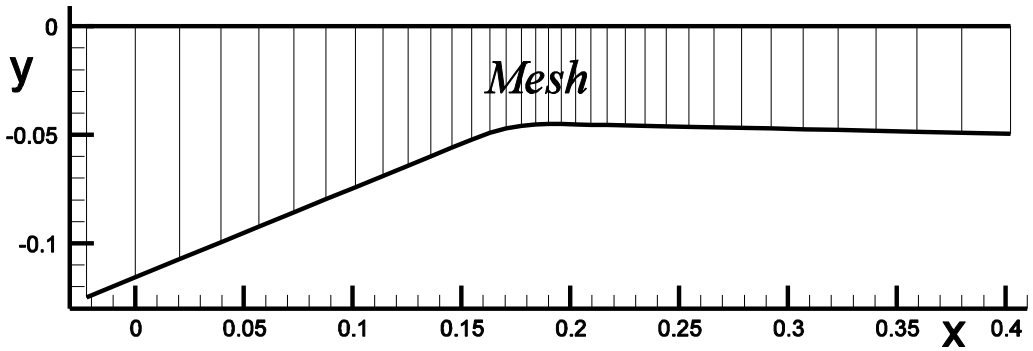

Figure 13.12 Stretched computational mesh

Initial Conditions

At $t = 0$ the flow is at rest.

$T = T_t = 531.7^o R$, the total temperature, $p = p_t = 2117.0\,lb/\,ft^2$, the total pressure, and $u = 0$.

Boundary Conditions

At the entrance, $x = 0$, the total temperature and pressure are held fixed.

At the exit, $x = L$, $p_{exit} = \frac{p_t}{3}$ as long as $M_{exit} < 1$.

Cases

Run each case below for 50 time steps. Show flow field results for surface pressure vs. x initially and for every 10 time steps.

1. No Shock Wave Case - The flow is uniformly at rest initially, except at the exit where the exit pressure is dropped to 1/3rd the total pressure value. This will start the flow moving. Use $\Delta t = 8 \left. \frac{\Delta x}{u + c} \right|_1$.
2. Stationary Shock Wave Case, - Use the result from Case (1) as the initial condition for this case, then increase the exit pressure to $p_{exit} = 0.67 p_t$. This will cause a shock wave to move into the diverging section of the nozzle. Use $\Delta t = 8 \left. \frac{\Delta x}{u + c} \right|_1$.
3. Moving Shock Case – Start with the solution from Case (2) and then increase the exit pressure by 67% ($p_{exit} \leftarrow 1.67 \times p_{exit}$) initially and thereafter hold it fixed. Use $\Delta t = \left. \frac{\Delta x}{u + c} \right|_1$

13.3.1 Solution Approach

Mesh Generation

We can modify the simple exponential mesh stretching formula discussed in Section 5.3.1 to generate the mesh. We start at the throat and place mesh points $x_i \quad for \quad i = i_{throat}, \cdots, I$, according to the following formula.

$$x_i = l + l \frac{e^{\kappa \frac{i - i_{throat}}{I - i_{throat}}} - 1}{e^{\kappa} - 1}$$

The parameter κ is again determined by Newton's method for finding the value for which $f(\kappa) = \Delta x_{\min} - (x_{i_{throat}+1} - l) = 0$. In our application $I = 33$ and $i_{throat} = 17$ for the finite difference mesh. The remaining mesh point locations for $i = 1, \cdots, i_{throat} - 1$ are obtained by reflection using those obtained above.

$x_i = L - x_{I+1-i}$

Boundary Conditions

See Section 12.3-5 for a general discussion of entrance and exit boundary conditions. For the present flow p_t and T_t are known at the entrance, which can be used as long as $M_{entrance} = \left. \frac{u}{c} \right|_{entrance} < 1$. These conditions are discussed in Section 13.2.5.2 for fully implicit boundary conditions at the entrance. We now discuss the implementation of semi-implicit boundary conditions at the entrance. From Section 13.2.5.2 we obtain, by replacing the fully implicit

approximation for the characteristic equation by the following semi-implicit approximation connecting mesh points (1) and (2).

$$\frac{p_1^{n+1}-p_1^n}{\Delta t}-\rho c\frac{u_1^{n+1}-u_1^n}{\Delta t}=-(u-c)\left(\frac{p_2^n-p_1^{n+1}}{\Delta x}-\rho c\frac{u_2^n-u_1^{n+1}}{\Delta x}\right)-\gamma p_1^{n+1}u_1^{n+1}\frac{S_2-S_1}{S_1\Delta x}$$

This equation can be written in "delta" law form by expressing $p_i^{n+1}=p_i^n+\delta p_i$ and $u_i^{n+1}=u_i^n+\delta u_i$ and then retaining the lowest order terms.

$$\frac{\delta p_1}{\Delta t}-\rho c\frac{\delta u_1}{\Delta t}+(u-c)\left(\frac{-\delta p_1}{\Delta x}-\rho c\frac{-\delta u_1}{\Delta x}\right)+\gamma(u_1^n\delta p_1+p_1^n\delta u_1)\frac{S_2-S_1}{S_1\Delta x}=$$
$$-(u-c)\left(\frac{p_2^n-p_1^n}{\Delta x}-\rho c\frac{u_2^n-u_1^n}{\Delta x}\right)-\gamma p_1^n u_1^n\frac{S_2-S_1}{S_1\Delta x}=R_3$$

Defining $\lambda_3=(u-c)\dfrac{\Delta t}{\Delta x}$ and then combining this equation for δu_1 and δp_1 with those obtained from the total pressure and density relations given in Section 13.2.5.2, we obtain the following matrix equation

$$\underbrace{\begin{bmatrix} 1 & -\left.\frac{\partial\rho}{\partial u}\right|_1 & 0 \\ 0 & -\left.\frac{\partial p}{\partial u}\right|_1 & 1 \\ 0 & -\rho c(1-\lambda_3)+\Delta t\gamma p_1^n\frac{S_2-S_1}{S_1\Delta x} & 1-\lambda_3+\Delta t\gamma u_1^n\frac{S_2-S_1}{S_1\Delta x} \end{bmatrix}}_{A'}\begin{bmatrix}\delta\rho_1^{n+1}\\ \delta u_1^{n+1}\\ \delta p_1^{n+1}\end{bmatrix}=\Delta t\underbrace{\begin{bmatrix}0\\0\\R_3\end{bmatrix}}_{\bar{\mathrm{R}}}$$

After inverting the above 3x3 matrix equation $A'\delta V_1^{n+1}=\Delta t\bar{\mathrm{R}}$ to determine δV_1^{n+1} we can use the matrix S^{-1} given earlier in Section 13.2.3 to find $\delta U_1^{n+1}=S^{-1}\delta V_1^{n+1}$. Note that some matrix inversion procedures may have difficulties if $u=0$, which implies that $-\left.\frac{\partial\rho}{\partial u}\right|_1=0$ and $-\left.\frac{\partial p}{\partial u}\right|_1=0$. However, the matrix can be easily inverted to obtain

$$\begin{bmatrix} \delta\rho_1^{n+1} \\ \delta u_1^{n+1} \\ \delta p_1^{n+1} \end{bmatrix} = \begin{bmatrix} 0 \\ \dfrac{\Delta t R_3}{-\rho c(1-\lambda_3) + \Delta t \gamma p_1^n \dfrac{S_2 - S_1}{S_1 \Delta x}} \\ 0 \end{bmatrix}$$

At the exit δU_I^{n+1} can be found as in Section 13.2.2.1.

Solution Algorithm

The Gauss-Seidel solution algorithm for the Quasi 1-D Euler Equations, using the results of Section 13.2.2.3, can be written as follows. See also Section 11.5

$$\bar{\mathrm{A}}_i \delta U_i^{n+1} = \Delta U_i^n - \bar{\mathrm{B}}_i \delta U_{i+1}^{(*)} - \bar{\mathrm{C}}_i \delta U_{i-1}^{(**)}$$

$$\text{with } \Delta U_i^n = -\frac{\Delta t}{S_i}\left(\frac{S_{i+1/2} F_{i+1/2}^n - S_{i-1/2} F_{i-1/2}^n}{\Delta x} \right) + \Delta t Q_i^n$$

The 3x3 block element matrices $\bar{\mathrm{A}}_i$, $\bar{\mathrm{B}}_i$ and $\bar{\mathrm{C}}_i$ are defined in Section13.2.3.1. The matrix $\bar{\mathrm{A}}_i$ can be inverted to determine δU_i^{n+1} for each i using the procedure outlined in Section 11.3.

13.3.2 Solutions

Case (1) Solution

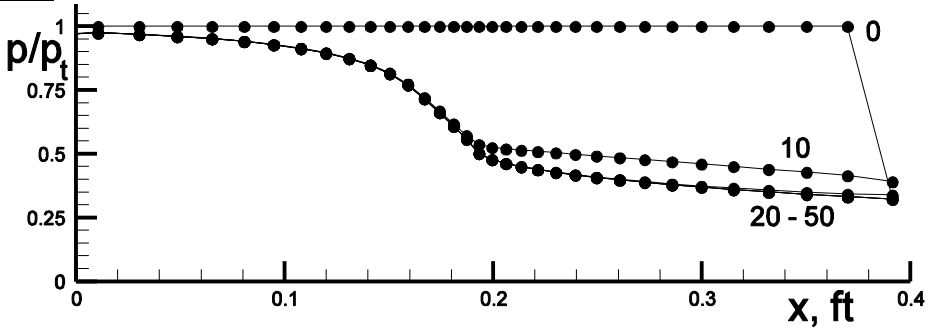

Figure 13.13 Case (1), pressure vs. x, converging to steady state

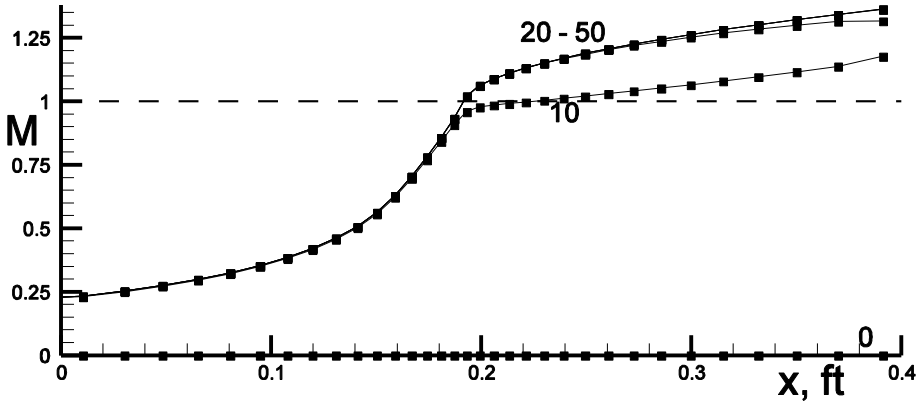

Figure 13.14 Case (1), Mach number vs. x, converging to steady state

Case (2) Solution

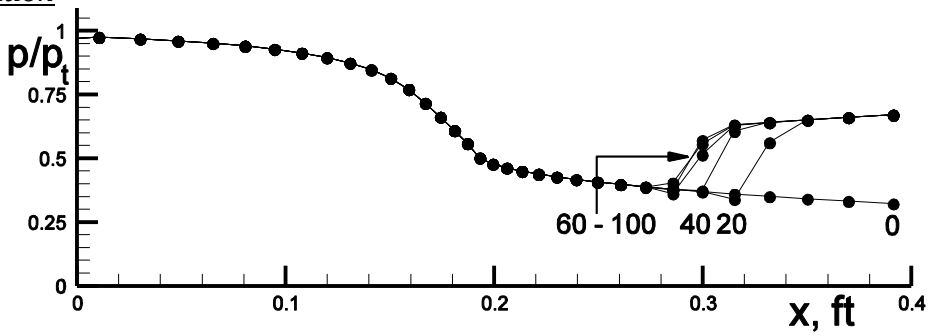

Figure 13.15 Case (2), stationary shock wave solution, 100 time steps

Case (3) Solution

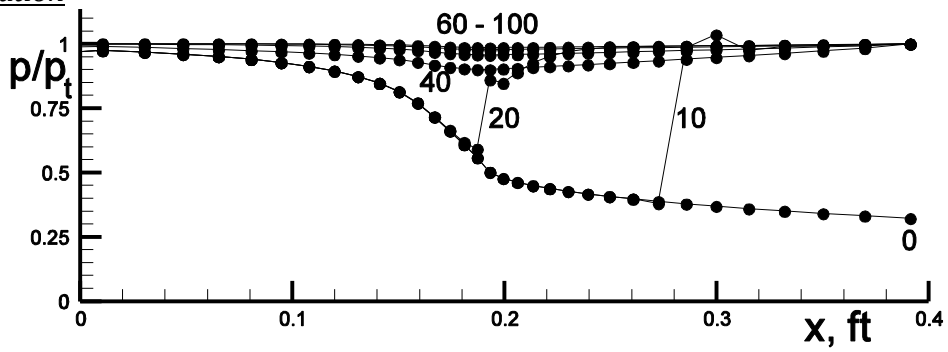

Figure 13.16 Case (3), moving shock wave, converging toward no flow solution

13.4 Piston Flow Problem

Exercise (4): Consider a piston moving down a closed cylinder, at speed V_p into pressurized air initially at rest. Calculate the flow within the cylinder until the piston stops and starts to reverse direction. Solve the Quasi 1-D unsteady Euler equations with an explicit method. Choose any of the methods from Chapter 9.

The equations to be solved are

$$\frac{\partial U}{\partial t}+\frac{1}{S}\frac{\partial FS}{\partial x}=0,$$

where

$$U=\begin{pmatrix}\rho\\ \rho u\\ e\end{pmatrix},\qquad F=\begin{pmatrix}\rho\\ \rho u^2+p\\ (e+p)u\end{pmatrix},\ S=\pi(D_p/2)^2$$

$$p=(\gamma-1)\rho\varepsilon \quad \text{and} \quad \varepsilon=c_vT=\frac{e}{\rho}-\frac{1}{2}u^2$$

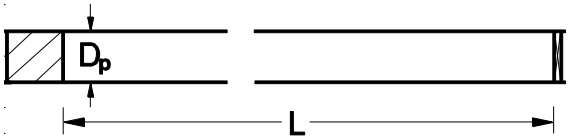

Figure 13.17 Piston within cylinder at t=0

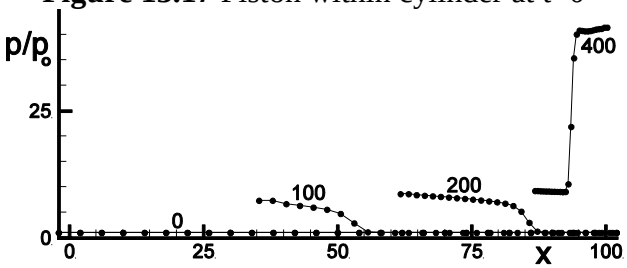

Figure 13.18 Pressure profiles, shock formation and reflection, during 400 time steps

Geometry and initial conditions

The piston diameter $D_p=0.1524m$ (6 inches), the piston mass $m_p=20kg$ and the length of cylinder is $L=100m$. The initial pressure of air within the cylinder is $p_0=10^6N/m^2$ and its temperature is $T=300^oK$. The piston is also initially at rest, but at t=0 a pressure of $p_b=10^7N/m^2$ is imposed upon the back surface of the piston and kept constant thereafter.

Cases

Use 25 finite volumes or 26 mesh points to span the length of the cylinder. Use CFL = 0.9.

(1) Run your program for 100 time steps with the back pressure set to $p_b=p_0$ (no flow case)

(2) Run your program for 400 time steps or until the piston stops and reverses. What is the maximum value of x_p, the distance the piston reaches after t=0 before reversing direction?

Mesh

The mesh should remain equally spaced between the front face of the piston and the end of the cylinder as the volume within the cylinder changes with movement of the piston. The moving Cartesian coordinate space (x,t) needs to be mapped into a stationary computational (ξ,τ) coordinate system. For convenience we will use the mesh index i to induce the metric for ξ. For the finite difference approach $\xi=1$ at $x=x_p$ and $\xi=I$ at $x=L$, where x_p is the location of the piston face and I is the number of mesh points spanning the flow volume.

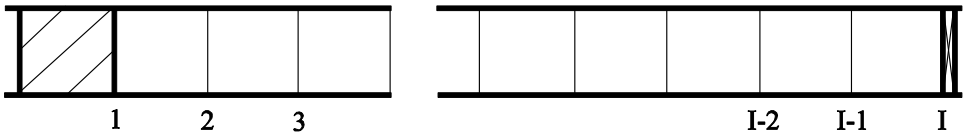

Figure 13.19a Finite difference mesh

For the finite volume approach $\xi=1+1/2$ at $x=x_p$ and $\xi=I+1/2$ at $x=L$, for the $I-1$ mesh volumes covering the flow volume.

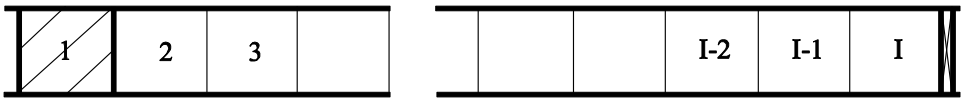

Figure 13.19b Finite volume mesh

The two meshes shown in Figures 13.19a and 19b appear the same, except that the mesh points are located at the cell faces for the finite difference approach and at cell centers for the finite volume approach

Transformations

The transformation between two moving coordinate systems was discussed in Section 7.4. The transformation considered there was two dimensional where as the one here is one dimensional. However, we can use the relations derived in Section 7.4 for the present case as well. Consider the following transformations. We look first at the finite difference mesh approach.

Finite difference approach

$$\xi = \xi(x,t) = 1 + \frac{x - x_p}{L - x_p}(I - 1), \quad \eta = y \quad and \quad \tau = t$$

The reverse transformations are

$$x = x(\xi,\tau) = x_p + \frac{\xi - 1}{I - 1}(L - x_p), \quad y = \eta \quad and \quad t = \tau$$

Then

$$d_{xy} = \frac{\partial x}{\partial \xi}\frac{\partial y}{\partial \eta} - \frac{\partial x}{\partial \eta}\frac{\partial y}{\partial \xi} = \frac{(L - x_p)}{I - 1} = \Delta x\,, \qquad \frac{\partial x}{\partial \eta} = 0\,, \qquad \frac{\partial y}{\partial \eta} = 1\,,$$

$$\frac{\partial x}{\partial \tau} = \frac{I - \xi}{I - 1}\dot{x}_p \qquad \text{and} \qquad \frac{\partial y}{\partial \tau} = 0\,, \qquad \text{where } \dot{x}_p = V_p\,, \quad \text{the speed of the piston.}$$

The transformed Euler equations become (using the definitions of Section 7.4)

$$\frac{\partial U'}{\partial t} + \frac{1}{S}\frac{\partial SF'}{\partial \xi} = 0\,, \quad \text{with} \quad U' = d_{xy}U = \Delta x U \quad \text{and}$$

$$F' = F\frac{\partial y}{\partial \eta} + U\left(\frac{\partial x}{\partial \eta}\frac{\partial y}{\partial \tau} - \frac{\partial y}{\partial \eta}\frac{\partial x}{\partial \tau}\right) = F - \frac{I - \xi}{I - 1}\dot{x}_p U$$

Upon simplifying,

$$\frac{\partial U\mathrm{V}}{\partial t} + \frac{\partial S(F - q_\xi U)}{\partial \xi} = 0\,,$$

Where V=SΔx and $q_\xi = \dfrac{I-\xi}{I-1}\dot{x}_p$ is the local speed of the mesh line ξ in the (x, y, t) coordinate system. The mesh point spacing Δx and volume V vary in time with piston movement.

Finite volume approach

$$\xi = \xi(x,t) = 1 + 1/2 + \frac{x - x_p}{L - x_p}(I-1), \quad \eta = y \quad and \quad \tau = t$$

The reverse transformations are

$$x = x(\xi,\tau) = x_p + \frac{\xi - 1 - 1/2}{I-1}(L - x_p), \quad y = \eta \quad and \quad t = \tau$$

These are the same relations given above with the exception that ξ is shifted by ½. The resulting differential equation is also the same with the exception that now $q_\xi = \dfrac{I + 1/2 - \xi}{I-1}\dot{x}_p$.

<u>Solution Algorithm</u>

The algorithm, in generic terms is

$$U_i^{n+1} = \left(\mathrm{V}_i^n U_i^n - \Delta t \frac{F'^n_{i+1/2} - F'^n_{i-1/2}}{\Delta\xi} \right) / \mathrm{V}_i^{n+1}$$

$$\text{where} \quad F' = S(F - q_\xi U) = S \begin{bmatrix} \rho q \\ \rho u q + p \\ e q + p u \end{bmatrix} \quad \text{and} \quad q = u - q_\xi$$

Because S is constant along the length of the channel, the equation can be rewritten as

$$\frac{\partial \Delta x U}{\partial t} + \frac{\partial (F - q_\xi U)}{\partial \xi} = 0$$

$$U_i^{n+1} = \left(\Delta x^n U_i^n - \Delta t \frac{F''^n_{i+1/2} - F''^n_{i-1/2}}{\Delta\xi} \right) / \Delta x^{n+1} \quad \text{with} \quad F'' = F - q_\xi U$$

<u>Piston speed and</u> Δx^{n+1}

At the start of the calculation $n = 0$, $x_p^n = 0$, $\dot{x}_p^n = 0$ and $\Delta x^n = L/(I-1)$. The acceleration of the piston during a time step Δt is $a_p^n = (p_b - p_1^n)A_p / m_p$, where $A_p = S$ is the area of the piston face, and the piston speed is approximated by $\dot{x}_p^{n+1} = \dot{x}_p^n + a_p^n \Delta t$. The location of the piston at time $(n+1)\Delta t$ is $x_p^{n+1} = x_p^n + \dfrac{1}{2}(\dot{x}_p^n + \dot{x}_p^{n+1})\Delta t$ and $\Delta x^{n+1} = (L - x_p^{n+1})/(I-1)$.

<u>Step size</u> Δt

The governing equation can be written in non-conservation form as

$$\frac{\partial U}{\partial t}+\frac{A-q_{\xi}I}{\Delta x}\frac{\partial U}{\partial \xi}=0, \quad \text{where} \quad A=\frac{\partial F}{\partial U} \quad \text{and here } I \text{ is the identity matrix.}$$

Therefore the time step size for step n is $\Delta t = 0.9 \min_{over\ all\ i}\left\{\frac{\Delta x^n}{\left|u_i - q_{\xi_i}\right| + c_i}\right\}$, where the CFL number has been chosen to be 0.9. (If the pure Steger-Warming is used as the algorithm, please see Section 9.6.1. The CFL number may need to be less than 0.9)

Boundary Conditions

The left and right boundaries are impermeable and "all you need is p". However, the left boundary, the piston surface, is moving and can perform work on the fluid. At either boundary the flux is given by

$$F_B'' = (F - q_{\xi}U)_B = \begin{bmatrix} 0 \\ p \\ pu \end{bmatrix}_B ,$$

At the left boundary, $u_B = \dot{x}_p$ and $p_B = p_2^n$. At the right boundary $u_B = 0$ and $p_B = p_I^n$ for the finite volume approach or $p_B = p_{I-1}^n$ for the finite difference approach.

Finite volume approach

The implementation of boundary conditions at solid walls is fairly simple for the finite volume approach. There is no need to define U_1^n or U_{I+1}^n or to use the interior point algorithm to define the flux at these boundaries. Simply use F_B' as defined above for the fluxes needed at $F_{i+1/2}'$, when $i=1$ or $i=I$. The piston and end wall faces are flux surfaces for this approach ensure that no mass, momentum or energy will cross these surfaces.

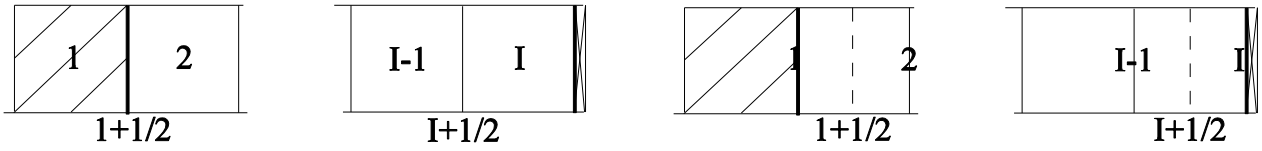

Figure 13.20a Finite volume mesh and **b** Finite difference mesh at boundaries

Finite difference approach

It would be difficult to determine U_1^n and U_I^n at the boundaries such that no mass, momentum or energy crossed through the piston or end wall surfaces. The simplest approach is the neglect the half a mesh point difference between the actual boundary location and the flux surfaces $F_{i+1/2}'$ to the left of mesh point $i=2$ and to the right of mesh point $i=I-1$ and then use the same boundary conditions as above for the finite difference approach. The flow volume will be shortened by one Δx, but conservation of mass, momentum and energy will be maintained.

Solution

Figures 13.21 and 22 compare the results computed using the Roe and Steger-Warming, Version (2) methods. The piston travels about 95m before reversing for the first time. The other algorithms presented in Chapter 9 yield similar results.

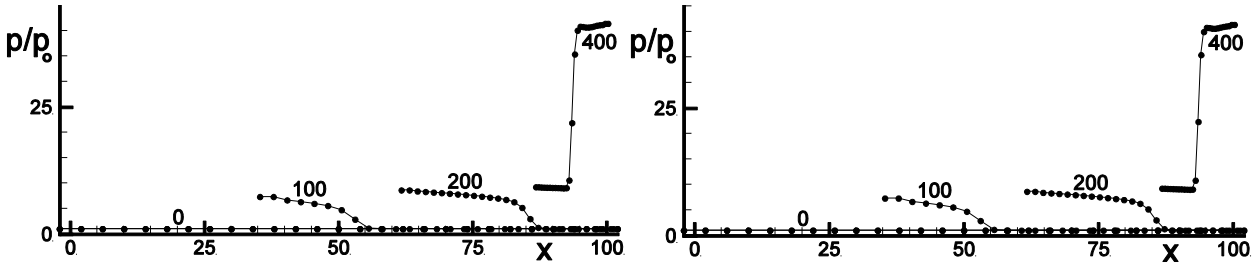

Roe Modified-Steger-Warming Version (2)

Figure 13.21 Pressure profiles, shock formation and reflection, during 400 time steps

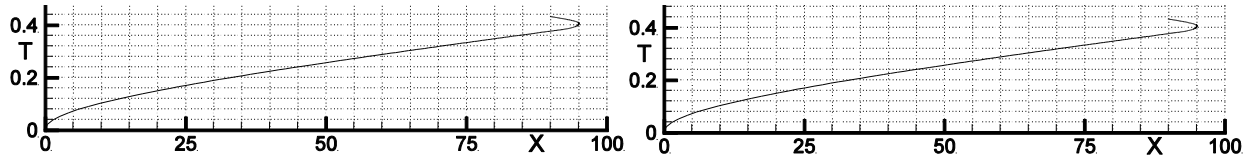

Roe Modified-Steger-Warming Version (2)

Figure 13.22 Piston locations in time, during 500 time steps

13.5 An Expansion Flow Problem

Exercise (5): Calculate Mach 3 flow over an expansion surface, sketched in Figure 13.23. Solve the 2-D Steady Euler equations with an explicit method. Choose any method from Chapter 9. Advance the solution by spatially marching it downstream to about x=1.2m. The computational solution can be compared with the analytic solution for Prandtl-Meyer expansion flow (see Anderson's *Fundamentals of Aerodynamics*).

The 2-D Steady Euler equations are (see also Section 2.7.2 and Section 2.8)

$$\frac{\partial F}{\partial x}+\frac{\partial G}{\partial y}=0,$$

where

$$F=\begin{pmatrix}\rho\\ \rho u^2+p\\ \rho uv\\ (e+p)u\end{pmatrix} \quad \text{and} \quad G=\begin{pmatrix}\rho v\\ \rho uv\\ \rho v^2+p\\ (e+p)v\end{pmatrix},$$

$$p=(\gamma-1)\rho\varepsilon \quad \text{and} \quad \varepsilon=c_v T=\frac{e}{\rho}-\frac{1}{2}(u^2+v^2)$$

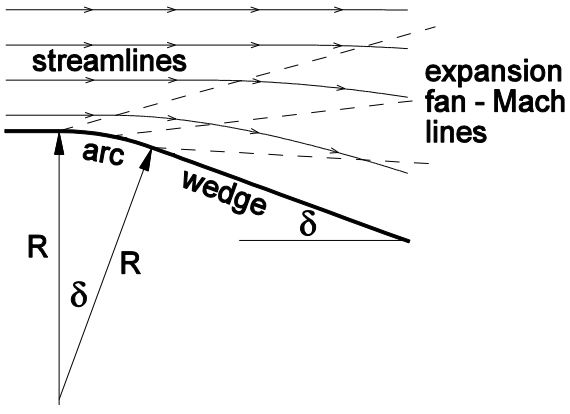

Figure 13.23 Flow over an expansion surface with R=1m. and $\delta=20^o$

Geometry and initial conditions

The surface geometry consists of a flat horizontal wall attached to a circular arc at x=0, followed by a flat wall sloping downward at an angle $\delta = 20^o$. The circular arc section has a radius of R=1m. The freestream flow ahead of the arc is at Mach 3, with pressure $p = 10^5 N/m^2$ and temperature $T = 300^o K$. The flow will remain supersonic and can be thus marched downstream over the expansion surface. The height of the flow field above the initial flat wall section is H=0.5m.

Mesh

The mesh and flow field Mach contours using the modified Steger-Warming Version 1 algorithm are shown in Figure 13.24. The CFL number was 0.9 and the initial solution, starting at about x=-0.245 (located 5 Δx upstream of x=0), was marched downstream for 32 spatial steps until approximately x=1.2. The circular arc section starts at x=0. The mesh is equally spaced vertically, containing about 27 mesh points between the body surface and y=H. The step size Δx, constant initially until the start of the circular arc, increases with x because of the expansion of the mesh vertically.

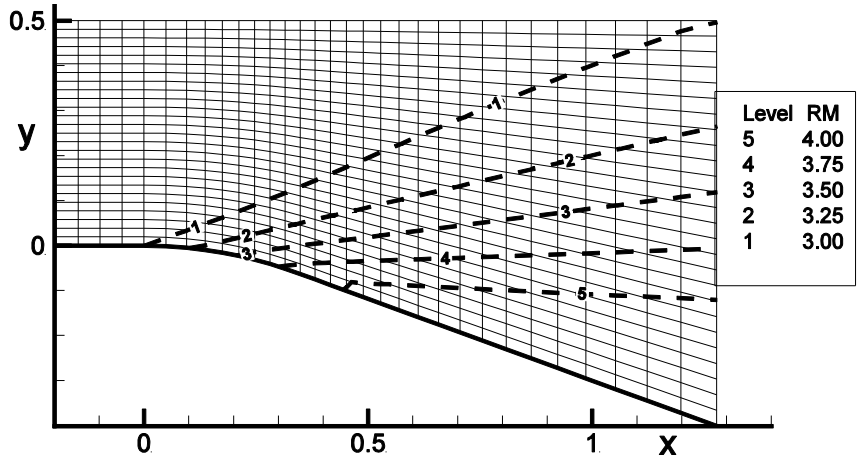

Figure 13.24 A 32 x 27 mesh and Mach contours from 3 to 4, MSW-(1)

Algorithm

The transformed equations to be solved are (see Section 7.3)

$$\frac{\partial F'}{\partial \xi} + \frac{\partial G'}{\partial \eta} = 0 \text{ with } F' = F\frac{\partial y}{\partial \eta} - G\frac{\partial x}{\partial \eta}, \quad G' = -F\frac{\partial y}{\partial \xi} + G\frac{\partial x}{\partial \xi}$$

The Flux vectors F' and G' are rotated to be normal to surfaces of constant ξ and η, respectively.

The generic algorithm for solving the above differential equation is

$$F'_{i+1,j} = F'_{i,j} - \Delta\xi \frac{G'_{i,j+1/2} - G'_{i,j-1/2}}{\Delta\eta}$$

The mesh shown in Figure 13.24 contains a set of vertical lines and a set that wraps about the surface. Therefore,

$$F'_{i,j} = F_{i,j}(y_{i,j+1/2} - y_{i,j-1/2}),$$

and

$$G'_{i,j+1/2} = -F_{i,j+1/2}(y_{i+1,j+1/2} - y_{i+1,j-1/2}) + G_{i,j+1/2}(x_{i+1,j+1/2} - x_{i+1,j-1/2})$$

As discussed in Chapter 7, the mesh indices i and j are used to determine the metrics ξ and η, such that $\Delta\xi = 1$ and $\Delta\eta = 1$, everywhere in the mesh.

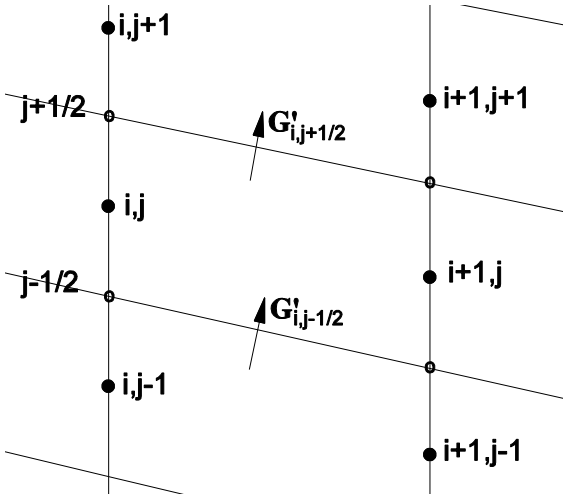

Figure 13.25 Mesh detail

If we define

$$\Delta y_{i,j} = y_{i,j+1/2} - y_{i,j-1/2}, \quad \Delta x_{i+1/2,j+1/2} = x_{i+1,j+1/2} - x_{i,j+1/2} \quad \text{and} \quad \Delta y_{i+1/2,j+1/2} = y_{i+1,j+1/2} - y_{i,j+1/2},$$

then the algorithm becomes

$$F_{i+1,j} = \left\{ F_{i,j}\Delta y_{i,j} - \Delta\xi \frac{G'_{i,j+1/2} - G'_{i,j-1/2}}{\Delta\eta} \right\} / \Delta y_{i+1,j},$$

where $$G'_{i,j+1/2} = \Delta x_{i+1/2} \left\{ G_{i,j+1/2} - F_{i,j+1/2} \frac{\Delta y_{i+1/2,j+1/2}}{\Delta x_{i+1/2,j+1/2}} \right\}$$

Determination of the step size Δx

The algorithm marches a vertical line of the solution downstream one spatial step at a time. The step size $\Delta x_{i+1/2}$ is found in a similar manner to Δt for unsteady flow problems. In the present case $\Delta x_{i+1/2} = 0.9 \min_{\text{over all } j} \left\{ \frac{\Delta y_{i,j}}{\max|\lambda|_{i,j}} \right\}$, where the CFL number has been chosen to be 0.9. To find the appropriate $\max|\lambda|_{i,j}$ we need to rewrite equation $\frac{\partial F'}{\partial \xi} + \frac{\partial G'}{\partial \eta} = 0$ in terms of Jacobian matrices as follows (see Section 2.7.2, where some adjustments need to made for the transformation from Cartesian to ξ, η coordinates)

$$A''\frac{\partial V}{\partial x} + B''\frac{\partial V}{\partial y} = 0 \quad \text{with} \quad A'' = T^{-1}AT, \quad B'' = T^{-1}(B - \varphi A)T, \quad T = \frac{\partial U}{\partial V}, \quad \varphi = -\frac{\partial y}{\partial \xi} / \frac{\partial x}{\partial \xi}$$

$$V = \begin{bmatrix} \rho \\ u \\ v \\ p \end{bmatrix}, \qquad A'' = \begin{pmatrix} u & \rho & 0 & 0 \\ 0 & u & 0 & \frac{1}{\rho} \\ 0 & 0 & u & 0 \\ 0 & \gamma p & 0 & u \end{pmatrix}, \qquad B'' = \begin{pmatrix} v' & \varphi\rho & \rho & 0 \\ 0 & v' & 0 & \frac{\varphi}{\rho} \\ 0 & 0 & v' & \frac{1}{\rho} \\ 0 & \varphi\gamma p & \gamma p & v' \end{pmatrix} \quad \text{and} \quad v' = v + \varphi u$$

Multiplying by the inverse of A'', we obtain

$$\frac{\partial V}{\partial x} + A''' \frac{\partial V}{\partial y} = 0, \text{ where } A''' = A''^{-1}B'' = \varphi I + \begin{pmatrix} \frac{v}{u} & \frac{-\rho v}{u^2 - c^2} & \frac{\rho u}{u^2 - c^2} & \frac{v}{u(u^2 - c^2)} \\ 0 & \frac{uv}{u^2 - c^2} & \frac{-c^2}{u^2 - c^2} & \frac{-v/\rho}{u^2 - c^2} \\ 0 & 0 & \frac{v}{u} & \frac{1}{\rho u} \\ 0 & \frac{-\rho c^2 v}{u^2 - c^2} & \frac{\rho c^2 u}{u^2 - c^2} & \frac{uv}{u^2 - c^2} \end{pmatrix} \text{ and } c^2 = \frac{\gamma p}{\rho}.$$

Notice this result is the same as that given in Section 7.2.2 with the minor exception that φ times the identity matrix has been added to the matrix A'''. Therefore the eigenvalues are

$$\lambda = \varphi + \frac{v}{u}, \quad \varphi + \frac{uv + c^2\beta}{u^2 - c^2} \quad \textit{and} \quad \varphi + \frac{uv - c^2\beta}{u^2 - c^2}, \text{ where } \quad \beta = \sqrt{(u^2 + v^2)/c^2 - 1},$$

and the matrices that diagonalize A''', S' and S'^{-1}, are the same as those given in Section 7.2.2.

Boundary Conditions

The top boundary of the mesh is far enough away from disturbances from the expansion surface at the lower boundary so that it will remain at freestream conditions during the calculation. Therefore, the flow variables there are set to the freestream values. Only pressure needs to be determined at the lower boundary. A single characteristic relation can be used to find pressure as described in Section 12.2.2.

Figure 13.26 shows the calculation after the solution has been advanced in space by Δx from x_n to x_{n+1}. The solution is now known at all interior points at both x_n and x_{n+1}. Pressure at wall point B needs to be determined so that a new spatial step downstream can be taken. The ξ_4 characteristic brings information to this point from the interior of the flow.

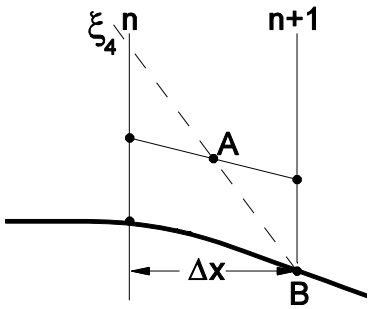

Figure 13.26 Boundary Condition

$$\frac{dp}{d\xi_4} - \frac{\rho u^2}{\beta}\frac{dv/u}{d\xi_4} = 0, \qquad \text{where} \qquad \frac{d}{d\xi_4} = \frac{\partial}{\partial x} + \left(\varphi + \frac{uv - c^2\beta}{u^2 - c^2}\right)\frac{\partial}{\partial y}$$

The slope of the characteristic path is $\varphi + \dfrac{uv - c^2\beta}{u^2 - c^2}$ and a finite difference equation approximation to the characteristic relation is

$$p_B \simeq p_A + \frac{\rho_A u_A^2}{\beta_A}\left(b'(x) - \frac{v_A}{u_A}\right), \qquad \text{with} \qquad \beta_A = \sqrt{\frac{u_A^2 + v_A^2}{c_A^2} - 1}, \qquad b'(x) = \frac{db(x)}{dx}$$

and the equation for the lower boundary given by $y = b(x)$. The location of point A is initially taken as lying half way between the two interior mesh points located next to the boundary. Point A lies on the line connecting these two interior points. Values for the flow variables at point A are first chosen to be the average values at these two points. Then the characteristic path using the values at point A is passed through point B and a new intersection point A is determined. New values are then interpolated for those at point A and the pressure at point B is then obtained from the difference approximation to the above characteristic relation.

Decoding the F vector

After the algorithm determines $F_{i+1,j}$ it must be decoded to find density, velocity and pressure. Let the elements of F be f_1, f_2, f_3 and f_4, then using relations similar to those of Section 2.4.3.7 for the stationary shock wave, let

$$m = f_1, \quad n = f_2, \quad v = f_3 / f_1 \quad \text{and total enthalpy } h = f_4 / f_1$$

As in Section 2.4.3.7, we can use the above relations and the perfect gas equation of state, $p = (\gamma - 1)\left(e - \frac{1}{2}\rho(u^2 + v^2)\right)$, to obtain a quadratic equation for the velocity u.

$$\underbrace{\left(\frac{1}{2} - \frac{\gamma}{\gamma - 1}\right)}_{a}u^2 + \underbrace{\frac{\gamma}{\gamma - 1}\frac{n}{m}}_{b}u + \underbrace{\frac{1}{2}v^2 - h}_{c} = 0$$

$$\text{with solution } u = \frac{-b - \sqrt{b^2 - 4ac}}{2a}$$

The solution with the minus sign before the square root sign was chosen to select the positive value for u, a a being negative. Finally $\rho = f_1 / u$ and $p = f_2 - f_1 u$

Note: We have solved a set of four equations – continuity, x and y momentum and energy. But we only need to solve three equations - continuity, and the two momentum equations – because total enthalpy, $h = (e + p)/\rho$, is constant throughout the flow. The energy equation was included for possible later extension to viscous steady flow.

Prandtl-Meyer theory

The Prandtl-Meyer function is given by (see Anderson's *Fundamentals of Aerodynamics*).

$$\nu(M) = \sqrt{\frac{\gamma+1}{\gamma-1}} \tan^{-1}\left(\sqrt{\frac{\gamma+1}{\gamma-1}(M^2-1)}\right) - \tan^{-1}\left(\sqrt{M^2-1}\right)$$

Where M is the local Mach number and $\nu(M)$ is the turning angle for a flow expanding from Mach 1 to Mach M. In our case $\vartheta = \nu(M) - \nu(M_\infty)$ is the turning angle required to expand the flow to Mach M from the freestream direction of the flow at Mach M_∞. Newton's method (see Section 5.3.1) can be used to find the Mach number corresponding to a point x along the lower surface. The equation to be solved via Newton's method is

$$f(M) = \nu(M) - \nu(M_\infty) - \vartheta = 0$$

where $\vartheta = -\tan^{-1}(b'(x))$. The pressure p at point x can be found by using the isentropic relation

$$p = p_T \left(1 + \frac{\gamma+1}{2} M^2\right)^{\frac{-\gamma}{\gamma-1}}, \qquad \text{where the total pressure} \qquad p_T = p_\infty \left(1 + \frac{\gamma+1}{2} M_\infty^2\right)^{\frac{\gamma}{\gamma-1}}$$

Solutions

Figure 13.27 compares the computed surface pressure with that from Prandtl-Meyer expansion theory. The first order Roe method was used in the calculation. The computed results follow, but lag slightly behind, the exact theory. All the explicit methods of Chapter 9 have very similar results.

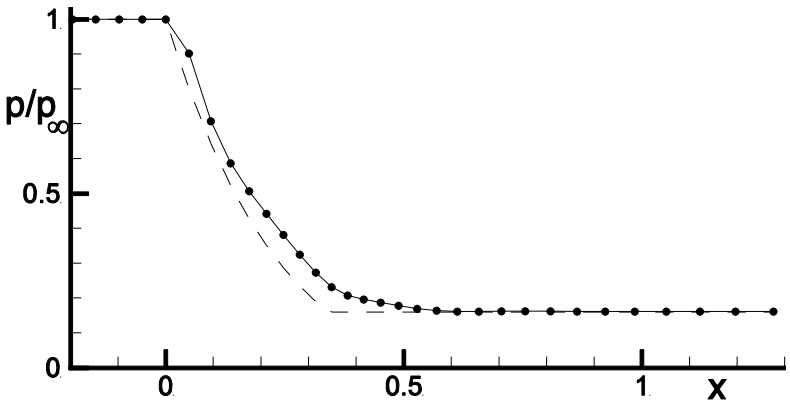

Figure 13.27 Surface pressure compared with Prandtl-Meyer theory, Roe

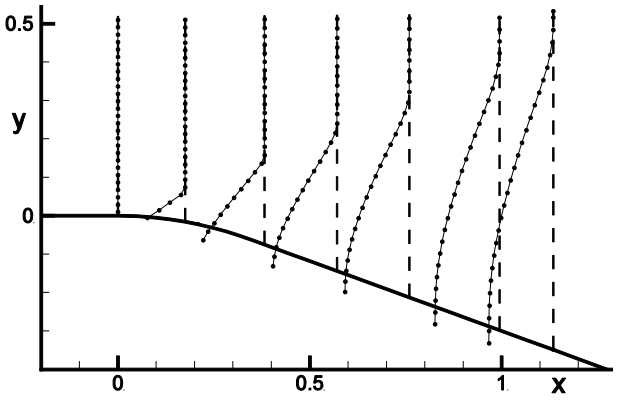

(a) MacCormack method

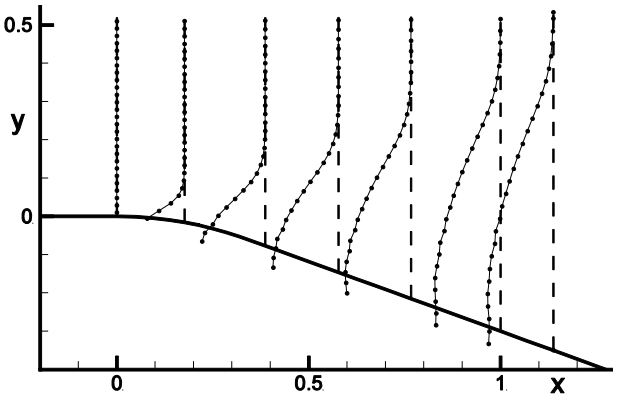

(b) Jameson method

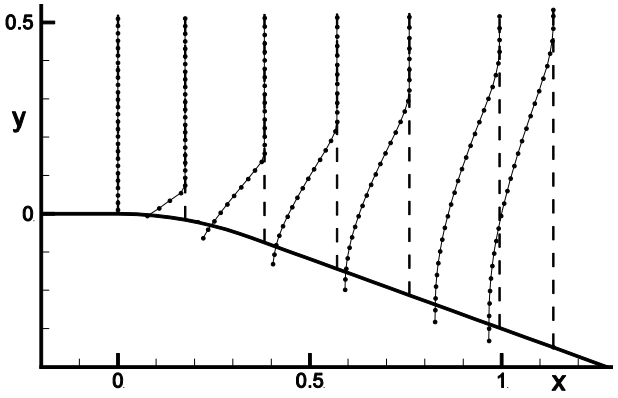

(c) Steger-Warming method

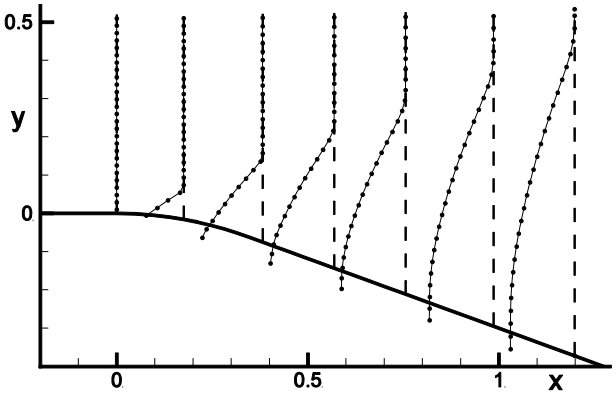

(d) Modified-Steger-Warming, version (1)

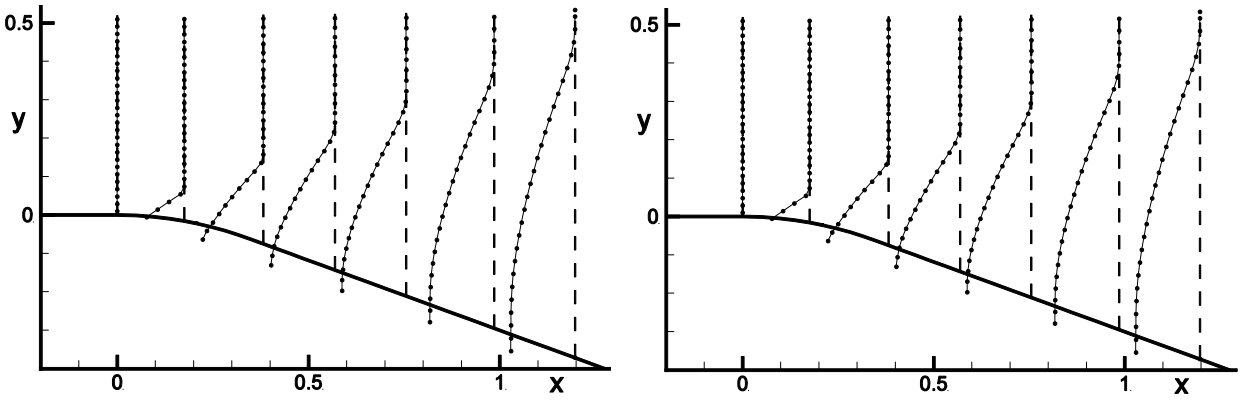

(e) Modified-Steger-Warming, version (2) (f) Roe method

Figure 13.28 Pressure profiles, at various downstream locations, for six explicit methods

Figure 13.28 shows the pressure profiles, at various downstream locations, computed by the MacCormack, Jameson, Steger-Warming, Modified-Steger-Warming versions (1) and (2) and Roe methods. The computed results by these methods for the relatively smooth expansion flow problem are very similar.

13.6 Compression Flow Problem

Exercise (6): Calculate Mach 3 flow over a compression surface, sketched in Figure 13.29. Solve the 2-D Steady Euler equations with an explicit method. Choose any method from Chapter 9. Advance the solution by spatially marching it downstream to about x=1.2m. The computational solution can be compared with the analytic solution for Prandtl-Meyer expansion flow (see Anderson's *Fundamentals of Aerodynamics*).

The 2-D Steady Euler equations are the same as those given earlier for the expansion flow problem. The flow field is shown in Figure 13.29 and a geometrical layout is sketched in Figure 13.30. Compression waves starting at the circular arc section of the surface coalesce to form a shock wave.

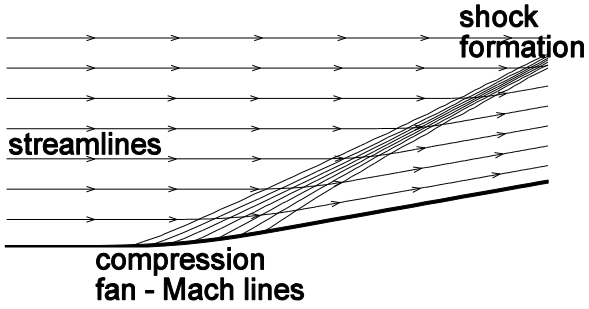

Figure 13.29 Compression surface flow

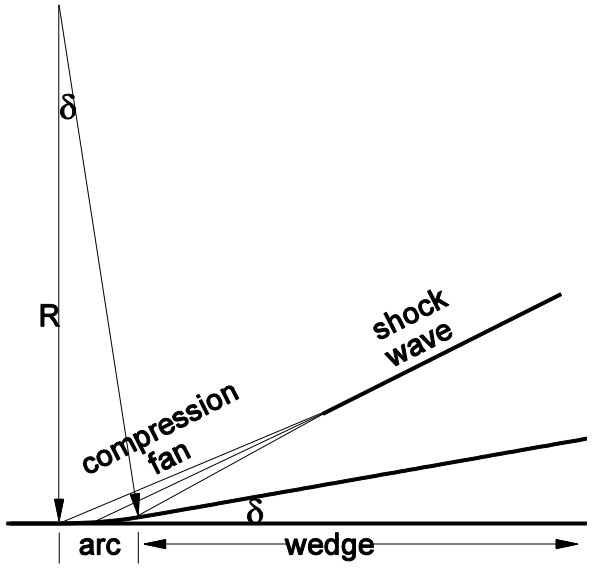

Figure 13.30 Compression surface geometry, with R=1m. and $\delta = 10^o$

Geometry and initial conditions

The surface geometry consists of a flat horizontal wall attached to a circular arc section at x=0, followed by a flat wall sloping upward at an angle $\delta = 10^o$. The circular arc section has a radius of R=1m. The freestream flow ahead of the arc is at Mach 3, with pressure $p = 10^5 N/m^2$ and temperature $T = 300^o K$. The flow will remain supersonic and can be thus marched downstream over the compression surface. The height of the flow field above the initial flat wall section is H=0.5m.

Mesh

The flow field Mach contours, using the modified Steger-Warming Version 2 algorithm, and a 101 x 28 mesh are shown in Figure 13.31. The CFL number was 0.9 and the initial solution, starting at about x=-0.245m (located 5 Δx upstream of x=0), was marched downstream for about 100 spatial steps until approximately x=1.2. The circular arc section starts at x=0. The mesh is equally spaced vertically, with about 27 mesh points between the body surface and y=H. The step size Δx is initially constant until the start of the circular arc and then decreases with x because of the compression of the mesh vertically to about x=0.5m, where the mesh begins to align itself to the forming shock wave. The mesh - shock wave alignment procedure is discussed below.

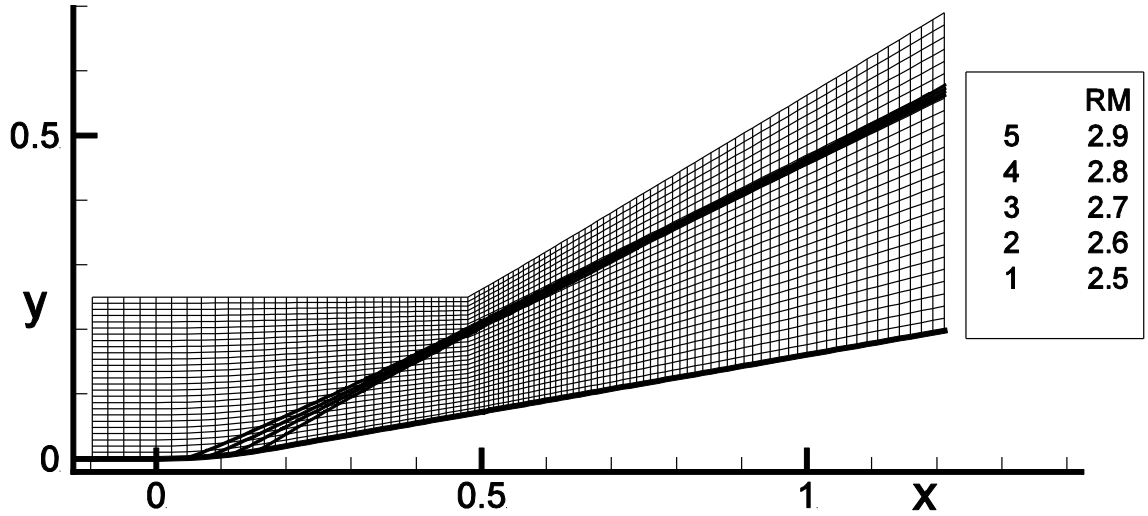

Figure 13.31 A 100 x 27 mesh and Mach contours, MSW-(2)

Mesh –Shock Wave Alignment

The heavy line in Figure 13.32 represents a section of the shock wave crossing through the line (or surface) of the known solution at x_n. This line also represents a line of the mesh with the j index given by $j = j_{shock}$. The shock wave angle is θ. The dashed line labeled ξ_2 is the characteristic path crossing the solution line to point S, located on the shock line downstream of x_n. The point C is the mesh point at $i = n$ and $j = j_{shock}$. In the present case $j_{shock} = 19$.

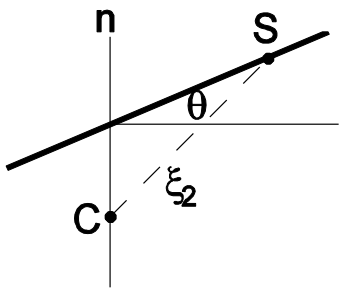

Figure 13.32 Mesh-shock alignment

The oblique shock relations for the steady Euler equations, devised in Section 2.4.3.6, are as follows, with subscript 1 representing the freestream side of the shock wave and the subscript 2 representing the flow across the shock wave. The components normal and tangential to the shock wave are in general $q_n = u\sin\theta - v\cos\theta$ and $q_t = u\cos\theta + v\sin\theta$, respectively. The freestream velocity has only an x component u_1.

$$\rho_2 q_{n2} = \rho_1 q_{n1} = \rho_1 u_1 \sin\theta$$

$$\rho_2 q_{n2}^2 + p_2 = \rho_1 q_{n1}^2 + p_1 = \rho_1 u_1^2 \sin^2\theta + p_1$$

$$\rho_2 q_{n2} q_{t2} = \rho_1 q_{n1} q_{t1} = \rho_1 u_1^2 \sin\theta\cos\theta$$

$$(e_2 + p_2) q_{n2} = (e_1 + p_1) q_{n1} = h\rho_1 u_1 \sin\theta = \left(\frac{\gamma}{\gamma - 1}\frac{p_1}{\rho_1} + \frac{1}{2}u_1^2\right)\rho_1 u_1 \sin\theta$$

These equations can be used to find a relation between $\sin\theta$ and p_2, plus the freestream conditions ahead of the shock wave, of the form

$$\sin\theta = \sqrt{\frac{\gamma p_2}{\rho_1 u_1^2} + \frac{\gamma - 1}{2\rho_1 u_1^2}(p_2 - p_1)}$$

Note that if $p_2 = p_1$ then the equation expresses the well known result for a Mach wave $\sin\theta = c_1 / u_1 = 1/M_1$. The ξ_2 characteristic relation, from Section 2.7.2, is

$$\frac{dp}{d\xi_2} + \frac{\rho u^2}{\beta}\frac{dv/u}{d\xi_2} = 0, \quad \text{where} \quad \frac{d}{d\xi_2} = \frac{\partial}{\partial x} + \frac{uv + c^2\beta}{u^2 - c^2}\frac{\partial}{\partial y}$$

The slope of the line joining points C and S is $\dfrac{uv + c^2\beta}{u^2 - c^2}$ and the finite difference approximation to the characteristic relation is

$$p_2 = p_C + \frac{\rho_C u_C^2}{\beta_C}\left(\frac{v_2}{u_2} - \frac{v_C}{u_C}\right), \quad \text{where} \quad \beta_C = \sqrt{\frac{u_C^2 + v_C^2}{c_C^2} - 1}$$

The variables with subscript 2 represent conditions at the shock wave point S. This last formula requires the ratio v_2 / u_2, which is at present unknown. But an iterative procedure can be used to converge to the conditions at point S, as follows.

(1) At $k = 0$ set $p_2^{(k)} = p_C$

(2) For $k = 1, 2, \cdots, 5$

$$\sin\theta^{(k)} = \sqrt{\frac{\gamma p_2^{(k-1)}}{\rho_1 u_1^2} + \frac{\gamma - 1}{2\rho_1 u_1^2}(p_2^{(k-1)} - p_1)}$$

$$\rho_2^{(k)} = (\rho_1 u_1 \sin\theta^{(k)})^2 / (\rho_1 u_1^2 \sin^2\theta^{(k)} + p_1 - p_2^{(k-1)})$$

$$q_{n2}^{(k)} = \rho_1 u_1 \sin\theta / \rho_2^{(k)}$$

$$q_{t2}^{(k)} = \rho_1 u_1^2 \sin\theta\cos\theta / \left(\rho_2^{(k)} q_{n2}^{(k)}\right)$$

$$u_2^{(k)} = \sin\theta\, q_{n2}^{(k)} + \cos\theta\, q_{t2}^{(k)}$$

$$v_2^{(k)} = -\cos\theta\, q_{n2}^{(k)} + \sin\theta\, q_{t2}^{(k)}$$

$$p_2^{(k)} = \frac{1}{2}\left\{ p_2^{(k-1)} + p_C + \frac{\rho_C u_C^2}{\beta_C}\left(\frac{v_2^{(k)}}{u_2^{(k)}} - \frac{v_C}{u_C}\right)\right\}$$

Note that in the last equation $p_2^{(k)}$ is under-relaxed (i.e., half the previous value is retained rather than accepting the new value entirely). At the end of 5 iterations θ is set to $\theta^{(5)}$. A decision has to be made on whether a shock wave is actually present and if the mesh line at $j = j_{shock}$ should be adjusted to be inclined at an angle of θ or not. Note that in Figure 13.31 the mesh is not adjusted until about x=0.5m. The mesh adjustment used herein was triggered by the following 10% criterion.

If $\theta \le 1.1\sin^{-1}(1/M_1)$, then no adjustment is made.
Otherwise, the mesh line from point C at n, j_{shock} to
the mesh point $n+1, j_{shock}$ is inclined at angle θ

The vertical mesh spacing Δy is set to $(y_{n+1,j_{shock}} - y_{n+1,1})/(j_{shock} - 1)$ and $y_{n+1,j} = y_{n+1,1} + (j-1)\Delta y$, for $j = 1, 2, \cdots, JL$.

Solutions

Figure 13.33 compares the computed surface pressure with that from Prandtl-Meyer expansion theory. The first order Roe method was used in the calculation. The computed results follow the exact theory fairly well, better than the solution given earlier for the expansion surface. All the explicit methods of Chapter 9 have fairly similar results for surface pressure.

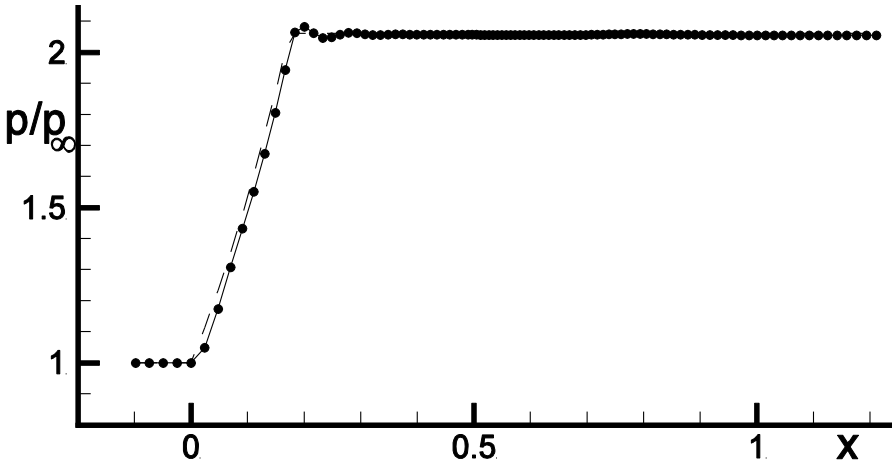

Figure 13.33 Surface pressure compared with Prandtl-Meyer theory, MSW-(2)

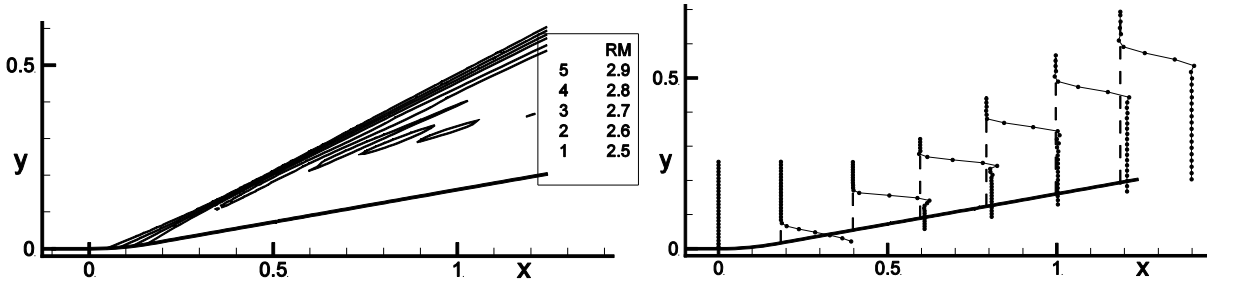

(a) MacCormack method

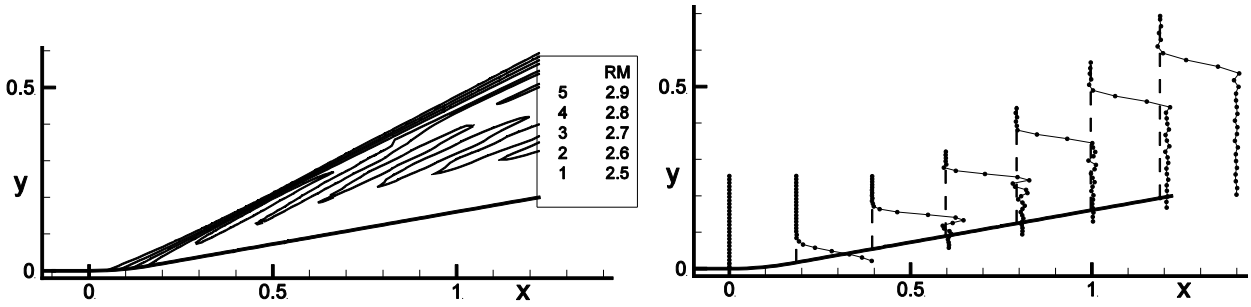

(b) Jameson method

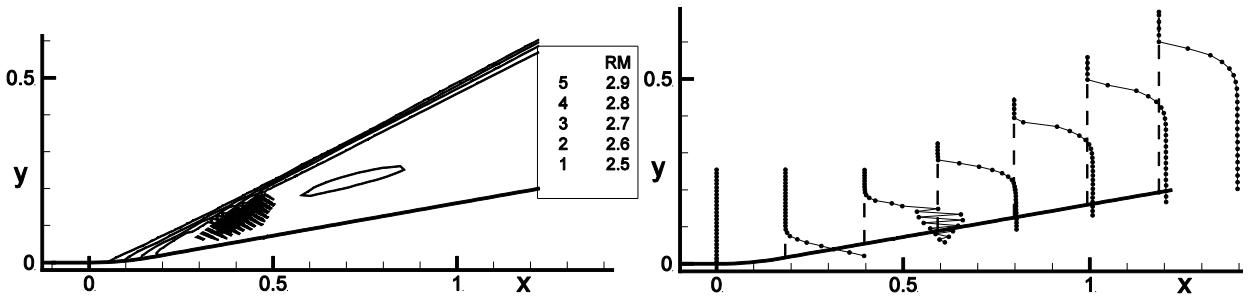

(c) Steger-Warming method

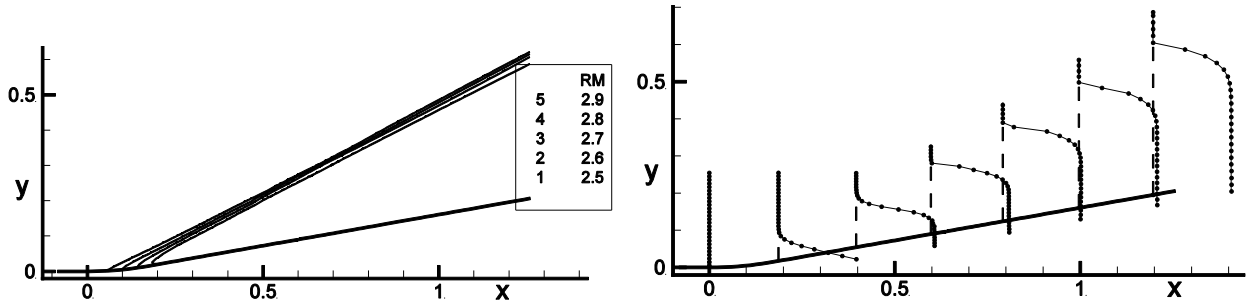

(d) Steger-Warming method, CFL=0.75

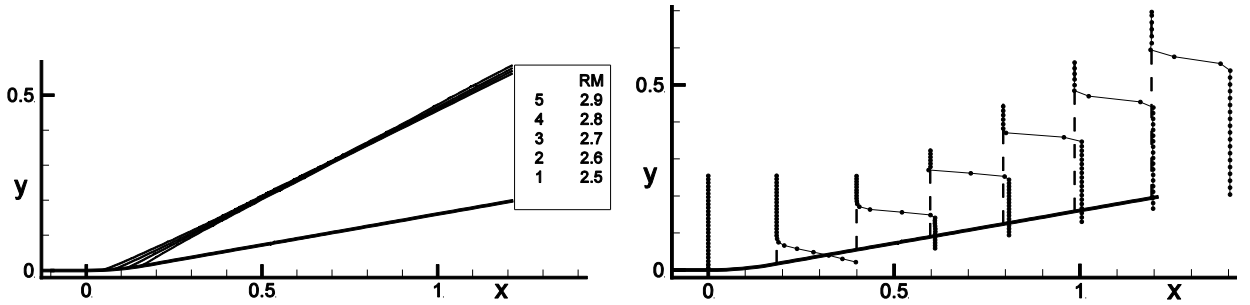

(e) Modified-Steger-Warming method, version (1)

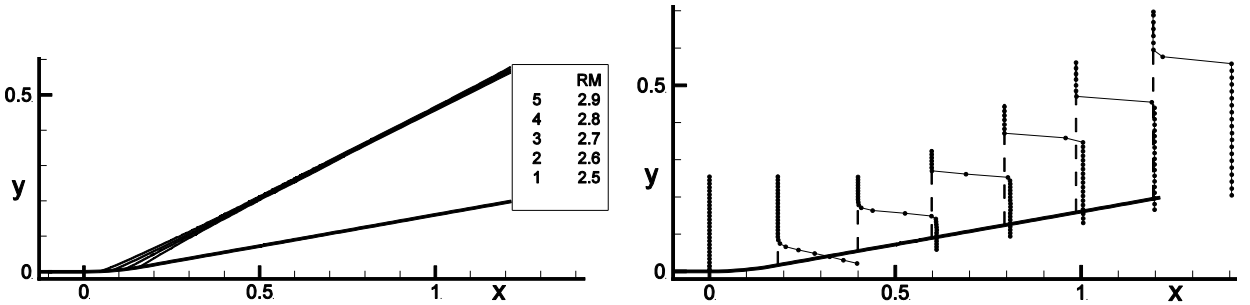

(f) Modified-Steger-Warming method, version (2)

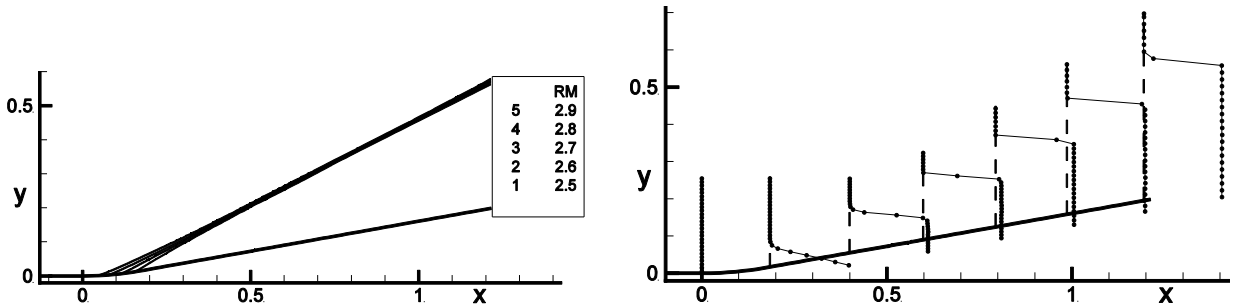

(g) Roe method

Figure 13.34 Flow field and pressure profiles at various downstream locations

Figure 13.34 (a) – (g) compare flow fields and pressure profiles, at various downstream locations, computed by the MacCormack, Jameson, Steger-Warming, Modified-Steger-Warming versions (1) and (2), and Roe methods. These methods were run using a CFL number of 0.9, unless otherwise noted in the figure captions. Mach contours from 2.5 to 2.9 are shown in the flow fields. It is clear that compression waves coalesce to form a shock wave in these figures.

Pressure oscillations are noticed in the MacCormack and Jameson methods, even with a smoothing term added of the form

$$G'_{i,j+1/2} \leftarrow G'_{i,j+1/2} - \varepsilon\left(F_{i,j+1} - F_{i,j}\right), \quad \text{with} \quad \varepsilon = \frac{1}{4}\frac{\left|p_{i,j+1} - p_{i,j}\right|}{\min\left\{p_{i,j+1}, p_{i,j}\right\}}\Delta y$$

The pure Steger warming method nearly failed at a CFL number of 0.9 near x=0.4m, but recovered downstream. No oscillations are present for this method at a CFL number 0.75, in accordance with the discussion in Sections 9.6.1 and 9.6.2. At CFL=0.75 the Steger-Warming method is smooth, even at the shock wave, caused by its relatively large numerical dissipation.

The Modified-Steger-Warming and Roe methods do fairly well with sharp pressure profiles at the shock wave, with the Roe method performing slightly better.